University of Nevada, Reno

# Mechanical Damping Properties of Carbon Nanofiber Reinforced Composites

A dissertation submitted in partial fulfillment of the requirements for the degree of Doctor of Philosophy in Mechanical Engineering

by

Joshua A. Varischetti

Dr. Jonghwan Suhr/ Dissertation Advisor

December, 2012

University of Nevada, Reno
Statewide • Worldwide

THE GRADUATE SCHOOL

We recommend that the dissertation
prepared under our supervision by

**JOSHUA A. VARISCHETTI**

entitled

**Mechanical Damping Properties Of Carbon Nanofiber Reinforced Composites**

be accepted in partial fulfillment of the
requirements for the degree of

**DOCTOR OF PHILOSOPHY**

Jonghwan Suhr, Ph.D., Advisor

Ronald Gibson, Ph. D., Committee Member

Shen-yi Luo, Ph. D., Committee Member

Yanto Shen, Ph. D., Committee Member

Qizhen Li, Ph. D., Graduate School Representative

Marsha H. Read, Ph. D., Dean, Graduate School

December, 2012

## Abstract

In this research an investigation of the damping enhancement achieved, utilizing carbon nano fibers (CNF) to epoxy resin is presented along with a corresponding model to predict damping performance. The addition of CNF fillers to the matrix allows for localized slip between the filler and the matrix on a nanoscale, wherein the matrix can de-bond from the CNFs, allowing the fillers to slip relative to the matrix; thereby, dissipating energy as frictional heat. Due to the nanoscale size of the filler, the specific surface area, of the CNF's, is very large when compared to traditional fiber reinforcement, this attribute allows small fractions of CNF fillers to have a large impact on the structural damping without any significant weight penalties. Moreover, once the composite returns to its undeformed configuration the interface between nano fillers and matrix will then re-establish the Van der Waals interactions that were broken to allow the slip. Thus, localized yet recoverable, frictional slip at the nano scale can be employed to significantly enhance strain dependent damping in composite structures wherein no permanent structural damage is evidenced. To better understand the damping response in CNF reinforced composites this study utilizes experimental and analytical approaches to develop modeling techniques that account for various fundamental attributes of high aspect ratio fillers, specifically the effect of filler aspect ratio, filler waviness, filler orientation relative to loading direction and the effect of multiple fillers on the damping performance and investigated in detail and corresponding modeling techniques are developed to address each of these factors in order to better predict the viscoelastic response of CNF reinforced composites. These models will be beneficial to address composite design while accounting for makeup, constituent properties, filler geometries, filler orientations, and their effective role in damping performance.

## Acknowledgments

First and foremost I would like to thank my advisor, Dr. Jonghwan Suhr, for providing me with many unique opportunities and challenges that have allowed me to grow and evolve throughout this process. None of this work would have been possible without his guidance, advice, and inspiration. Additionally, special recognition is due Dr. Ronald Gibson who has provided me with a tremendous amount of guidance and expertise in the development of the research presented here.

I would also like to thank the remainder of my dissertation committee members: Dr. Shen-Yi Luo, Dr. Yantao Shen, and Dr. Qizhen Li for taking the time to serve on my dissertation committee and providing all their advice throughout this process.

Additionally, I would like to thank my research colleague Jae-Soon Jang for all of his effort, guidance and support throughout the experimental portion of this study.

I would also like to acknowledge the financial support of Boeing, NSF-NUE and the mechanical engineering department at UNR for providing the funding to this study, without it none of this would have been possible.

Finally, I would like to thank my family and friends for providing the encouragement and support that kept me focused and sane throughout this experience.

## Table of Contents

## List of tables

## List of Figures

## 1. Introduction

Composite materials have long been utilized in a variety of engineering applications requiring the desirable combination of high strength and low weight[1], more recently a large amount of research in the area of nano scale materials has led to a notable interest in the use of nano scale fillers to a host matrix in order to create nanoscale composites for a variety of engineering applications[2-18]. Current fiber composites, having high modulus, and relatively low density, are well suited to a variety of engineering applications, however, the desirable combination of high strength and low mass, coupled with the non isotropic material properties, arising as a result of fiber orientation leads to complex vibrational responses which must be considered in composite design. Damping in engineered composites is of particular importance for vibration control and noise attenuation[1]. Lack of vibrational damping can result in a variety of issues ranging from limitations in structural performance, and fatigue wear, to the transmission of unwanted vibrations through composite structures to other aspects of engineering applications, resulting in sub optimal performance of integrated systems[5].

Current attempts to induce vibrational damping capability in composites range from the simplistic add-on type damping systems, to the vastly elaborate use of active control elements embedded in the composite. Presently, the most common approach is to utilize an add-on type damping treatment using a viscoelastic layer adhered to a base composite structure. The add-on type damping treatment can be seen in figure 1, where the viscoelastic layer is used with or without a stand-off layer and is constrained by another layer of material of similar rigidity to the base structure; when the base structure deforms, it results in shear deformation in the more compliant viscoelastic layer, this vibrational energy is then dissipated as heat. The use of a stand-off layer serves to increase the distance from the neutral axis, thereby increasing the amount of strain input to the viscoelastic layer as a function of the vibrational input of the base structure. This method, while effective at introducing damping, has several draw backs; the first being a substantial increase in weight due to the add-on damping treatment, which is in contradiction to the fundamental logic of using composites to minimize weight.

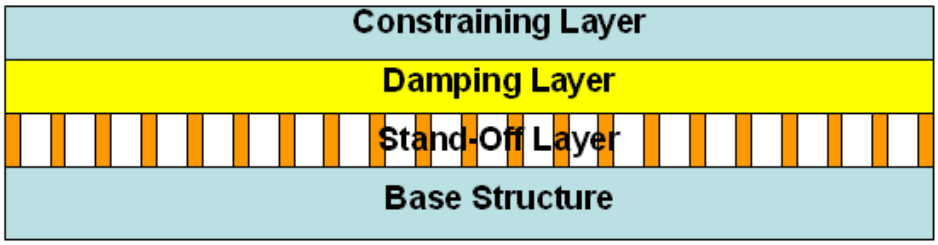


Figure 1: Schematic of conventional constraint layer viscoelastic damping treatment for composites.

Furthermore, the add-on type damping treatments have performance limitations with respect to operating temperature, frequency spectrum, and life span of the damping treatment[5]. The viscoelastic layers damp vibration across a relatively narrow frequency spectrum, therefore, to get broad spectrum damping for a variety of engineering applications often multiple viscoelastic layers are stacked in order to encompass broader frequency spectrum damping requirements that are often required of high performance composite materials. As well, viscoelastic damping treatments are also susceptible to reduced performance with increasing temperature changes; as a result, the effective operating environment of the damping treatment is often mismatched with the designed operating environments of the high performance composites they are intended to work with[16-18]. The viscoelastic damping layers are generally a soft polymer; this leads to issues of breakdown with exposure to ultra violet rays as well as temperatures changes[18].

Composites, by virtue of being engineered materials, are well understood in terms of analytical performance predictions; this is especially true of modern fiber composites, where detailed analytical techniques have been developed to accurately predict performance based on composite makeup, constituent properties, and geometry. This ability to predict as well as engineer performance with a high degree of certainty makes modern fiber composites especially attractive for critical applications where specific engineered performance is mandatory while over engineered additional weight is unacceptable. One of the key features of the ability to predict composite performance in modern fiber composites is the ability to accurately measure constituent material properties by modern test methods; this adds to the level of confidence in composite material performance. Conversely, the material properties of nano scale constituents, while thought to be superior to micro and macro scale composite constituents, present a large

challenge in terms of measuring constituent material properties, primarily due to the size of the constituents, conventional material testing is impractical, this can lead to large performance gaps when compared to analytical predictions. Current design and analysis techniques make use of several simplifying assumptions including perfect cylindrical or spherical geometry of the nano scale constituents, such as nanotubes and nano particles, along with perfect bonding of the fillers and matrix to achieve design models which can only predict trends in performance, but lack the ability to engineer specific performance. It is well understood that there is inherent error in making these assumptions, and a fair amount of research has focused on the specific implications of these assumptions with respect to the structural material properties of the nanostructured composites, however there is currently not a damping design model capable of predicting composite damping performance based on nano constituent properties and nano constituent geometry, which is one aim of this dissertation research.

This research is designed to study damping response in carbon nanofiber (CNF) composites utilizing dynamic mechanical analysis to measure viscoelastic response, which can then be directly translated in to damping performance. Through the use of the viscoelastic correspondence principle the modulus can be separated in to the storage and loss components seen in equation 1, where the complex modulus (E*) is comprised of the storage modulus (E') and the loss modulus (E"). Assuming linear viscoelastic relationships necessary to use the complex modulus the loss factor (η) can be calculated as the loss modulus divided by the storage modulus η=(E" / E'). The use of linear viscoelastic analysis such as the complex modulus with low strain experimental studies, maintaining linear viscoelasticity, allows for a detailed study of the fundamental material response of the nanocomposites which can then be used to develop better modeling techniques to be used in engineering nanocomposite performance for specific applications.

$$E^* = E' + iE'' \tag{1}$$

In addition to the low strain amplitude experimentation and analysis this study also uses large strain amplitude experimentation and analysis in an effort to better characterize and interpret the behavior of

nanoscale composites at realistic strain levels necessary for application. Additionally, large strain investigations are beneficial in understating the non-linear stick-slip frictional sliding, which when coupled with random distribution of fillers seen in most nano composites results in a strain dependent damping response. The use of large strain investigations provides insight as to the nature of the strain dependent damping response seen in the CNF filled nanocomposites; in addition to the ability to derive specimen properties which offer insight to the macro scale behavior of the nanocomposites which need to be better characterized in order to develop the next generations of engineered nanocomposites.

Specifically, this research looks at the effect of filler geometry, as well as multiple fillers in characterizing damping performance in nanostructured composites, which can then be utilized as nano-enhanced matrix properties for conventional fiber composite designs. In parallel to the damping characterization, detailed modeling has been developed to address filler geometry, both aspect ratio and waviness of high aspect ratio fillers, and the strain dependent nature of the damping enhancement seen with the addition of CNF. The overall objectives of this research are to gain fundamental insight as to the viscoelastic response of CNF enhanced nanocomposites, while developing corresponding modeling techniques which may be used to better understand viscoelastic response in nanocomposites and ultimately engineer a desired performance based on constituent makeup and properties.

## 2. Damping in nano structured composites with carbon nano fibers

This research is designed to study damping response in carbon nanofiber (CNF) composites. The addition of CNF fillers to the matrix allows for localized slip between the filler and the matrix on a nanoscale, wherein the matrix can de-bond from the CNFs, allowing the fillers to slip relative to the matrix; thereby, dissipating energy as frictional heat[2]. This phenomena, though not visually observed, has been validated through the use of acoustic emission (AE) measurements. Utilizing AE it is possible to witness this acoustically, essentially hearing the CNF filler de-bond from the matrix. This evidence coupled with the enhanced damping performance achieved in experimental work, provides the basis for the hypothesizes and experimental work presented here. Due to their size, the specific surface area of CNF, are very large when

compared to traditional fiber reinforcement, this attribute allows small fractions of CNF fillers to have a large impact on the structural damping without any significant weight penalties. Moreover, once the composite returns to its original configuration the interface between nano fillers and matrix will then re-establish the Van der Waals interactions that were broken to allow the slip. Thus, localized yet recoverable, frictional slip at the nano scale can be employed to significantly enhance strain dependent damping in composite structures wherein no permanent structural damage is evidenced.

A review of the literature indicates that, while there has been considerable work done on the use of nano scale fillers to enhance damping of polymer resins[2-16], yet there has been little work done on the use of nano scale fillers to structural fiber reinforced composite laminates, which would be required for practical application purposes where damping in composite structures is a matter of growing importance for a variety of engineering applications. Furthermore, while damping improvements have been shown empirically throughout literature utilizing nanoscale fillers, there remains a lack of analytical techniques that can be used to engineer nanostructured composite materials. The stick-slip nature of the damping enhancement is well understood and referenced[4,7] Additionally, there has been work done on the use of nano scale fillers, for damping purposes, with active control[8], however, these methods incur significant penalties in the form of weight and power requirements, as well as a limited window of damping effectiveness such as temperatures or frequencies. In this research the focus was on passive damping systems that have negligible weight penalties while providing desired damping enhancement over a wide range of application frequencies and operating temperatures. Additionally, comprehensive modeling techniques will be explored with the aim of developing useful modeling techniques, which could be used to engineer specific structural and damping performance in nano structured composites.

## 2.1 Experimental approach

This research utilizes a series of experiments, designed progressively, to demonstrate the feasibility of damping enhancements, through the use of CNF inclusions to polymer resins, and ultimately to structural

application grade carbon fiber reinforced laminate composite structures. Materials were pre-screened using Dynamic Mechanical Analysis (DMA) and dynamic cyclic testing to validate damping enhancement hypotheses, prior to their inclusion in structural carbon fiber reinforced laminate composite beams; which were then tested using dynamic cyclic testing as well as beam vibration testing per ASTM E-756-05. Pre-screening of the material characteristics was done with DMA first because it provides a relatively fast and economical way to test a small sample and quickly validate hypothesis. Dynamic cyclic testing was followed to further validate it at realistic loading conditions. Afterwards, CNF included carbon fiber epoxy composite panels were fabricated and their damping performance was evaluated in both beam vibration tests and dynamic cyclic testing.

## 2.2 Materials and fabrication

Materials used include: Miller Stephenson EPON™ Resin 862 along with EPIKURE™ 9553 curing agent purchased from Miller Stephenson Inc., plain weave carbon fiber mat (an average fiber diameter of 8μm) from Fiberglast Inc., graphitized CNF with dimensions of 200-500nm in diameter and 10-40μm in length as well as smaller diameter CNF having dimensions of 80-200nm in diameter and 10-40μm in length from Nano Amorphous Materials Inc.

All samples were fabricated using Miller Stephenson EPON™ Resin 862 along with EPIKURE™ 9553 curing agent at a weight ratio of 100:16.84. The epoxy resin was first treated to an air release agent BYK-500 that was added at a weight fraction of 0.01% to assist in removing air bubbles from the epoxy. The epoxy resin was then degassed under vacuum to remove air entrapped in the epoxy. For the nano filler included samples, the filler was then added at appropriate amounts to reach desired loading, and dispersed with a high speed mechanical shear mixer. Graphitized carbon nano fiber was selected as the filler in the investigation, which was purchased from Nano Amorphous Materials Inc. (Houston, TX), and used as received. The primary (large) CNFs have 200-500nm in diameter and 10-40μm in length, resulting in nominal aspect ratios of 71. After incorporation of the filler the curing agent was added and dispersed with a high speed shear mixer again. Upon completion of the resin preparation the epoxy resin was poured into

silicone molds and cured in a pressure tank at 90psi and room temperature for 24 hours. Post curing was done in an oven at 100°C for 1 hour. This process can be seen in figure 2. All of the dynamic cyclic test samples created by this fabrication process were of the dimensions shown in Figure 3(a), as per ASTM D638-99. All of the DMA samples created were of the dimensions shown in figure 3(b) as recommended by Gibson[1]. For the investigation 3 different loadings of CNF dispersed epoxy composites were fabricated; 0, 3, and 5wt% were considered. Theses loadings (up to 5wt%) were chosen in this project considering the manufacturing difficulties resulting from dramatic increase in viscosity and agglomeration of CNFs at higher loadings. Note that it was possible to successfully fabricate up to 8ply carbon fiber reinforced epoxy composite panels with uniformly dispersed 5wt% CNF inclusions through VARTM technique seen in figure 2(b).

(a)

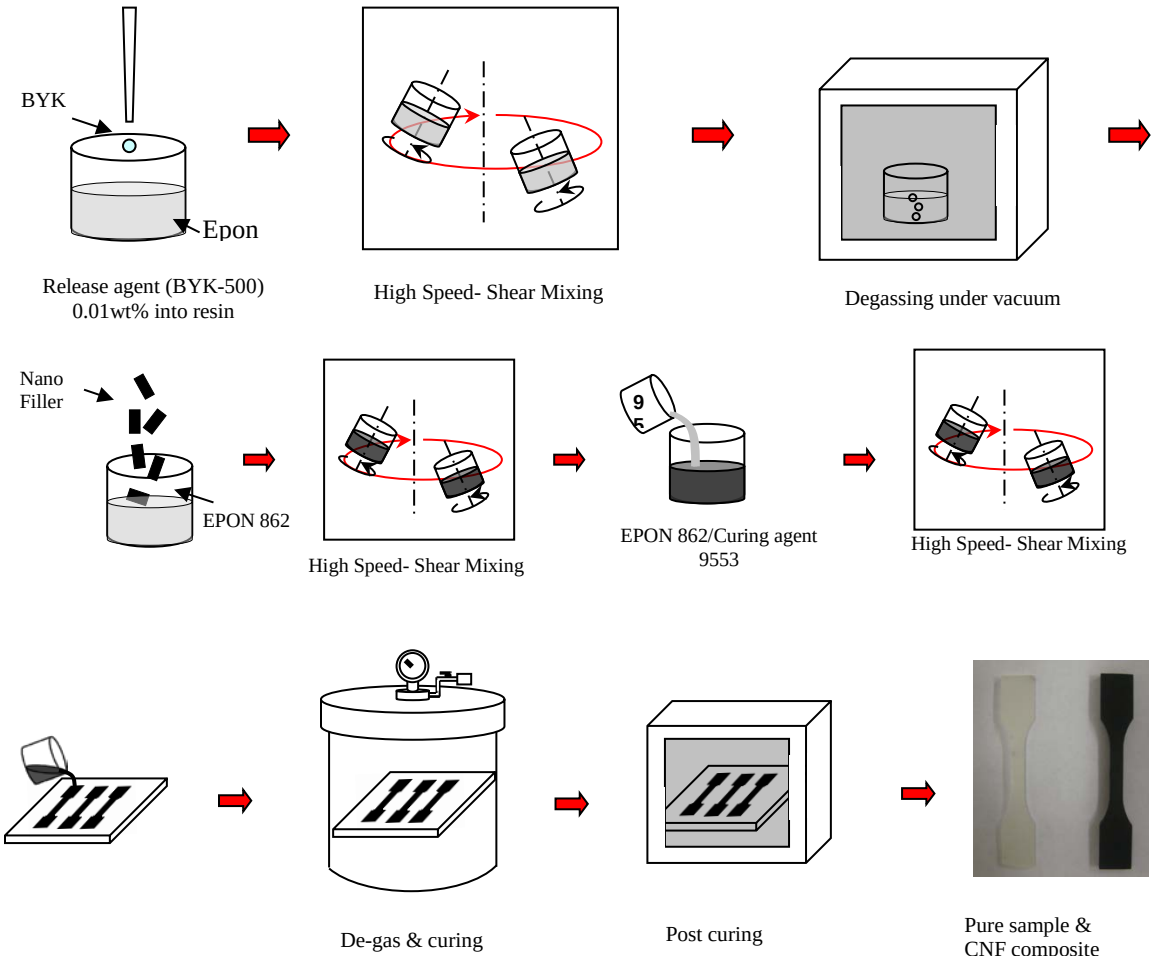

(b)

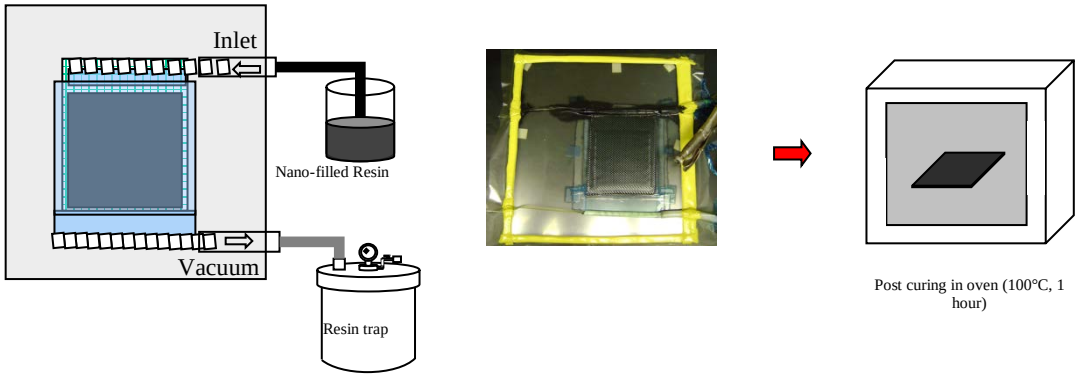


Figure 2: (a) Schematic of manufacturing process used to fabricate tensile DMA / dynamic cyclic test coupons of pure epoxy and CNF included epoxy resin (b) Fabrication of CNF included carbon fiber composite panels using VARTM.

(a) Dynamic Cyclic Testing Sample dimension

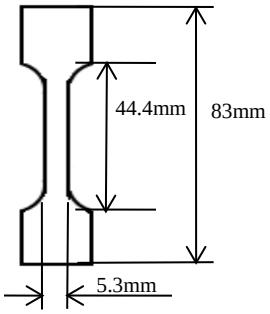


(b) DMA Sample Dimensions

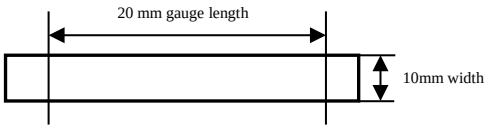


* Thickness 1.5mm

Figure 3: (a) Sample dimensions of dynamic cyclic testing tensile dog bone specimens, and (b) Sample dimensions of DMA tensile beam specimens.

Surface morphology of the prepared samples was investigated using SEM characterization to ensure uniform dispersion of the nano fillers; as can be seen in figure 4, good dispersion of fillers (down to individual nanofiber dispersion level) was achieved though the developed fabrication process.

Fabrication of carbon fiber reinforced composite samples was completed using a vacuum assisted resin transfer molding process (VARTM). Samples were constructed of plain weave carbon fiber mat purchased from Fiberglast Inc. Laminates were constructed in 4, 6, and 8 ply configurations. The composite lay up

was prepared on a flat glass mold and vacuum bagged. The resin was prepared as in figure 2(a). The resin was then infused into the composite by means of vacuum assistance and held under vacuum for 24 hours to complete the initial cure. Following the initial cure the samples were removed from the mold and placed in an oven for post curing at 100°C for a period of 1 hour, after which, beam specimens with desirable dimensions were cut from the composite panel. This fabrication process is illustrated in figure 2(b). Fabrication validation included SEM imagery, where uniform dispersion through the entire thickness of the fracture surface was observed, along with good dispersion quality, down to the individual CNF level as can be seen in figure 4(b).

(a)

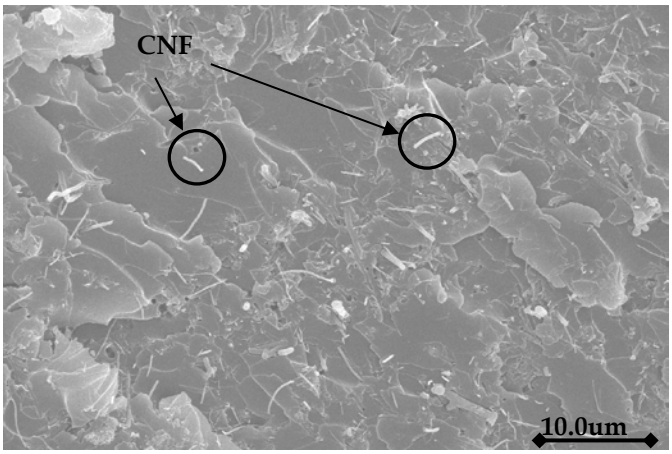


(b)

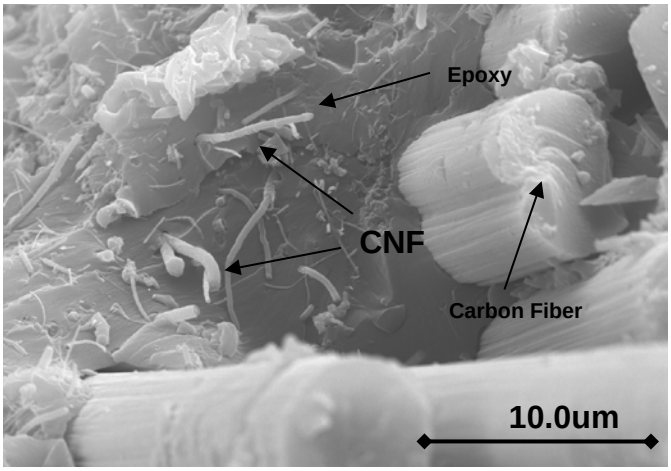


Figure 4: (a) SEM characterization of 5wt% CNF included epoxy fracture surface showing well dispersed CNF with no agglomeration, and (b) SEM characterization of 3wt% CNF included carbon fiber composite fracture surface, showing uniform distribution and good dispersion of CNFs in the resin matrix.

Prior to conducting any experimentation, a differential scanning calorimetry (DSC) test was run on the baseline EPON 862 sample to check that the glass transition temperature was in line with published references, which would ensure the fabrication of samples was in accordance with acceptable standards. This test was run using a TA instrument DSC. Figure 5 shows the reference $T_g$ of the baseline EPON 862 was found to be 98°C, this is in range with the Miller-Stephenson published specification sheet

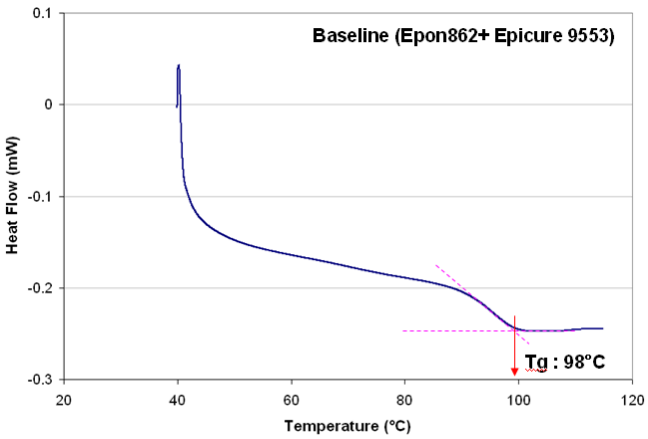


Figure 5: DSC results for baseline EPON 862.

A static tensile test was also performed to ensure that the Young's modulus of the prepared baseline samples (~3.0GPa) was in agreement with published values (~2.9GPa). As well this static test provided the limits of the linear elastic range that would later be used in the testing protocol to ensure all testing was performed in the linear elastic range.

## 2.3 DMA results and analysis

The initial investigation began with a DMA analysis as part of the pre-screening process to test the hypothesis. Additionally, the DMA allowed investigation of the temperature dependence of the damping enhancement provided though CNF inclusions to the matrix, a temperature swept DMA analysis was performed using a PerkinElmer Diamond Lab DMA instrument; as well the same instrument was used to investigate the frequency dependence of the results. For the DMA analysis all samples were prepared in the

manner shown in figure 2(a), to the same dimensions shown in figure 3(b). All DMA tests were conducted in flexural mode on at least 3 samples of each type of material for each test condition. Results presented here are the average response of the tested samples at a given test condition for a specified material type. DMA temperature sweeps were run from -50°C - 130°C at a temperature ramp of 5°C/min to investigate the nature of any temperature dependence on the viscoelastic properties of the CNF included resin. All tests were run at 1Hz. Figure 6(a) shows the storage modulus as a function of temperature, it can be seen from the temperature sweep that the storage modulus increases with increased loading of CNF across the entire temperature range. Additionally, in a temperature controlled environment at 25°C, the storage modulus increases by 16.5% for the 5wt% CNFs-epoxy sample over the baseline. All DMA testing was done with no initial strain in tension mode. Figure 6(b) shows the temperature sweep for the loss modulus, it can be seen that up to $T_g$, across the entire useful temperature spectrum, increased CNF loading results in an increased loss modulus. For a reference, the loss modulus at 25°C is found to have an increase of 32% for the 5 wt% CNF-epoxy sample over the baseline, this is slightly lower, yet comparable to the results found using dynamic cyclic testing at room temperature that will be presented in a subsequent section. Figure 6(c) shows comparable temperature dependent behavior for the loss factor as a function of temperature. Adding CNFs increases the loss factor up to $T_g$, however, increasing loading of CNF is not indicative of increased loss factor as is measured at the 25°C reference the 3wt% has marginally improved damping over the 5wt% specimens. This is because the 3wt% CNF-epoxy sample has lower storage modulus when compared to 5wt% CNF-epoxy sample. Yet, both the 3wt% and 5wt% samples show an improvement of 25% relative to the baseline sample. Furthermore, Figure 6(c) shows that with an increase in CNF loading the $T_g$ is also increased. This indicates that the CNF provides additional reinforcement to the epoxy matrix.

(a)

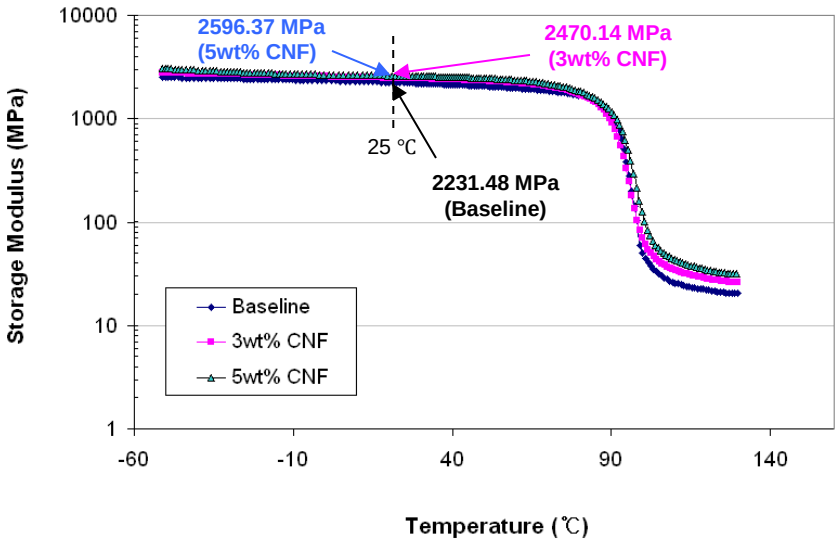
2596.37 MPa
(5wt% CNF)
2470.14 MPa
(3wt% CNF)
25 ℃
2231.48 MPa
(Baseline)
Baseline
3wt% CNF
5wt% CNF
Storage Modulus (MPa)
10000
1000
100
10
1
-60
-10
40
90
140
Temperature (℃)

(b)

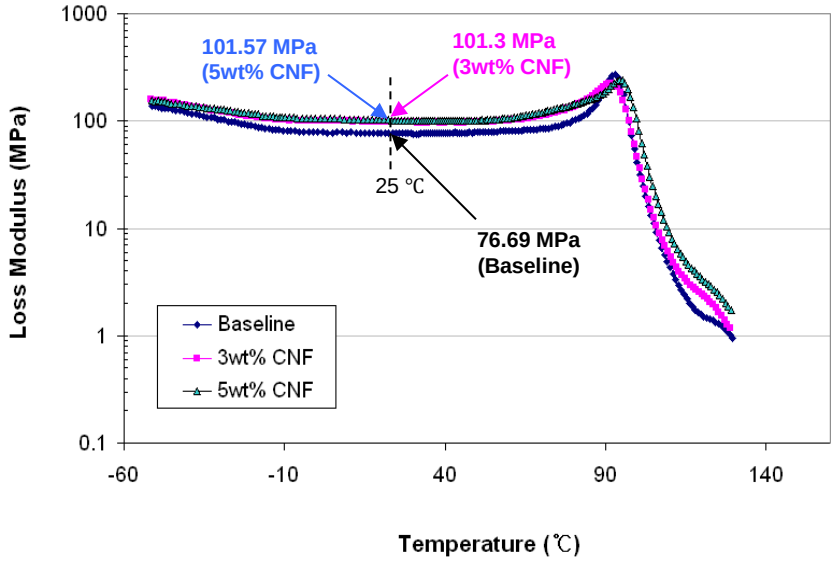
101.57 MPa
(5wt% CNF)
101.3 MPa
(3wt% CNF)
25 ℃
76.69 MPa
(Baseline)
Baseline
3wt% CNF
5wt% CNF
Loss Modulus (MPa)
1000
100
10
1
0.1
-60
-10
40
90
140
Temperature (℃)

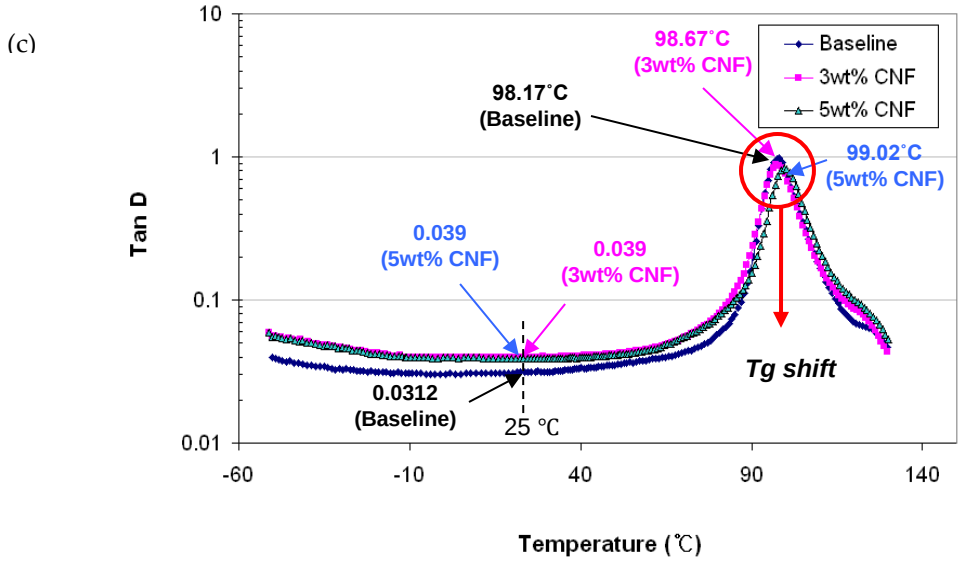


Figure 6: (a) DMA Temperature sweep results for storage modulus as a function of temperature for varying amounts of CNF in resin, and (b) DMA Temperature sweep results for loss modulus as a function of temperature for varying amounts of CNF in resin, and (c): DMA Temperature sweep results for loss factor as a function of temperature for varying amounts of CNF in resin. All tests were performed at 1Hz.

To investigate the frequency dependence of the damping enhancement attained through CNF additions, frequency sweeps were conducted on the same samples constructed in identical manner as for the temperature sweep tests. For the frequency sweep tests, the temperature was held constant at 25°C; while the test frequency was swept from 0.1Hz to 100Hz. Figure 7(a) shows the frequency independence of the storage modulus. It can be seen that the storage modulus is increased for all loadings of CNF; as well there is no evident frequency dependence in the storage modulus for this enhancement. Figure 7(b) shows the frequency sweep on the loss modulus. It can be seen that there exists a slight decreasing trend in the loss modulus with an increase in frequency, however the addition of CNF does provide enhancement of 29% in comparing the 5wt% sample to the baseline at a frequency of 1Hz. The frequency dependent decrease is not fully understood, but hypothesized to be related to the intrinsic relaxation time of the composite for heat energy dissipation out of the material. It should be noted that generally it provides more time for the frictional energy to get dissipated at lower frequency. Being derived from the storage and loss modulus; the loss factor expectedly exhibits the same frequency dependence trends seen in the loss modulus, the results

seen in figure 7(c) mirror the results seen in the loss modulus; as there was no noticeable frequency dependence in the storage modulus behavior.

(a)

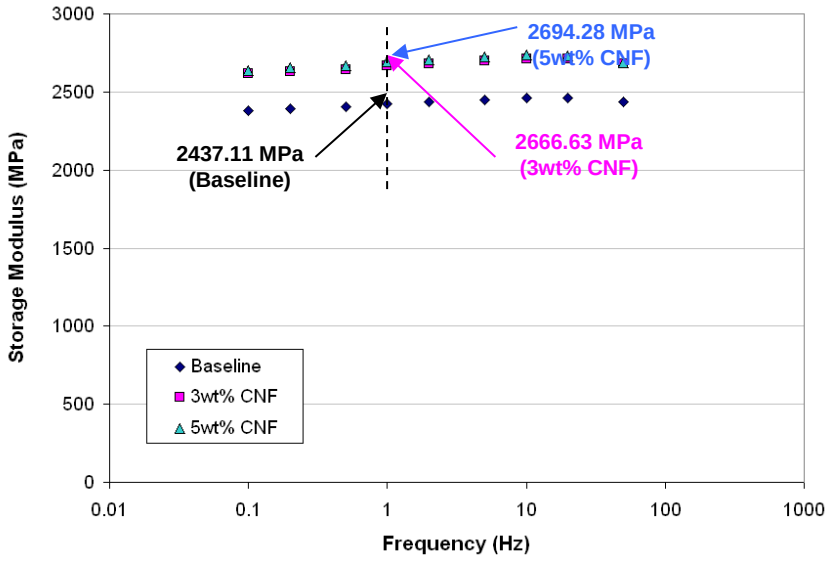


(b)

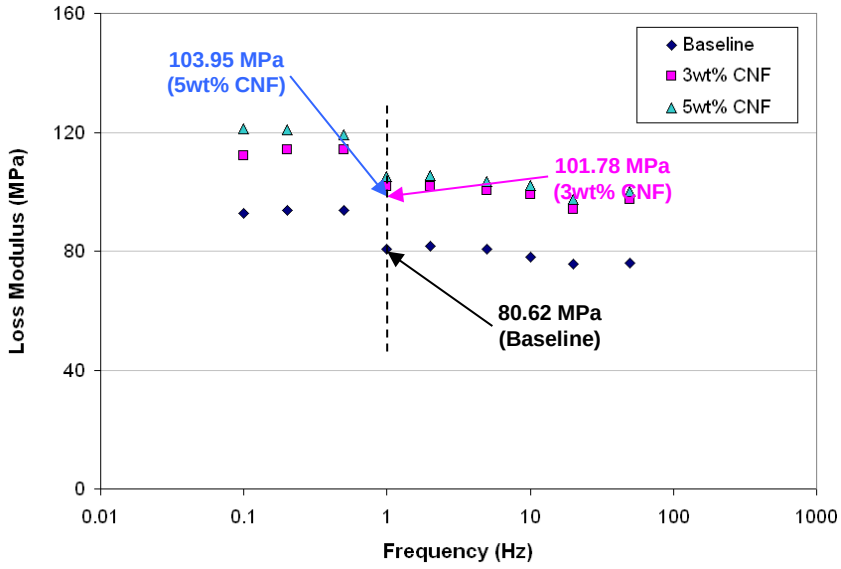

(c)

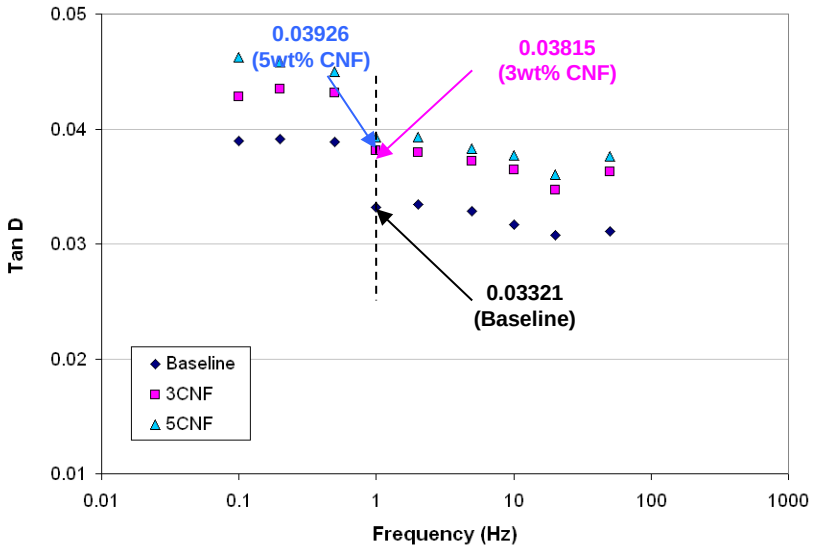


Figure 7: (a) Frequency sweep results for storage modulus as a function of frequency for 0, 3 and 5wt% CNF epoxy resin, (b) Frequency sweep results for loss modulus as a function of frequency for 0, 3 and 5wt% CNF epoxy resin, and (c) Frequency sweep results for loss factor as a function of frequency for 0, 3 and 5wt% CNF epoxy resin. All tests were conducted at constant temperature of 25°C.

## 2.4 Dynamic cyclic testing results and analysis

To further validate results obtained from DMA tests and investigate the effect of strain dependent behavior on damping, dynamic cyclic testing was performed at more realistic strain levels on larger specimens that would reflect a more practical application scenario. Dynamic cyclic testing was done on a BOSE Electroforce 3300 dynamic cyclic testing set-up. All testing was done at a frequency of 1 Hz. To ensure that all testing was done under tension, an initial tensile strain of 0.6% was applied to accommodate dynamic strain amplitudes of up to 0.5% while still maintaining tension in the sample. This was necessary due to the larger stresses and strains utilized in the dynamic cyclic testing, coupled with the specimen geometry necessary for the test; as buckling was a concern if there were compressive strains of this magnitude in the samples. To investigate the strain dependence of the damping enhancement 4 different dynamic strains were selected, 0.25%, 0.5%, 0.75%, and 1%. This test condition can be visualized in figure 8. The strain range considered for testing was limited to the linear elastic range as determined through a static tensile test. It should be noted that the measured loss factors reported are not necessarily intrinsic material properties, due to the initial applied strain, necessary to maintain tension in the sample,

however, the improvements are intrinsic of the material as all testing was subject to the same discipline. All testing was done at room temperature. The testing machine was used to calculate the constituent parts of the complex modulus denoted E* = (E' + iE") where E', the in plane component, represents the storage modulus, and E", or the out of plane component, represents the loss modulus. The damping loss factor was then calculated as the loss modulus over the storage modulus.

The initial static tensile test was used to determine the linear elastic range of the material for consideration in dynamic cyclic testing. The initial static tests performed on 0, 3, and 5wt% CNF included samples show the linear elastic range of all samples to be identical up to 2% strain. Also note that Young's modulus of CNF included epoxy composites is slightly increased as the CNF loading increases, clearly showing the reinforcement effect of CNFs for the composites.

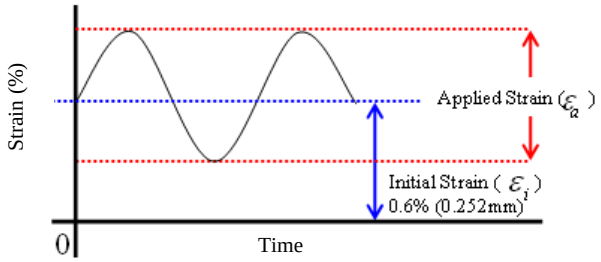


Figure 8: Schematic of dynamic cyclic testing conditions, showing initial applied strain to accommodate applied strain amplitudes of up to 1% applied strain, while maintaining tension in the specimen.

Dynamic cyclic testing was performed for at least 3 samples of each type at each specific strain; results presented are the average response of the test data. Figure 9 shows the results of the dynamic cyclic testing on the matrix samples, from figure 9(a) we see the addition of CNF provides an increase in the storage modulus of 7%; we can also see that the effect of enhancement on the storage modulus is slightly decreasing as strain increases, indicating activation of frictional sliding between CNFs and epoxy matrix due to interfacial failure. Figure 9(b) shows improvements in the loss modulus of up to 80%; it can be seen that higher loading of CNFs – epoxy exhibits increases in loss modulus at all strain levels investigated, furthermore, it is observed that the increase in loss modulus shows a strain dependent behavior, consistent with the stick slip nature of the damping due to frictional sliding of the filler relative to the matrix. Essentially, as the strain increases, more of the filler is activated in the frictional slip mechanism that

generates mechanical damping. This behavior is due to the random dispersion of the filler in the matrix, as the strain is increased more of the CNFs experience a critical shear stress relative to individual orientations that allow them to slip relative to the matrix.

(a)

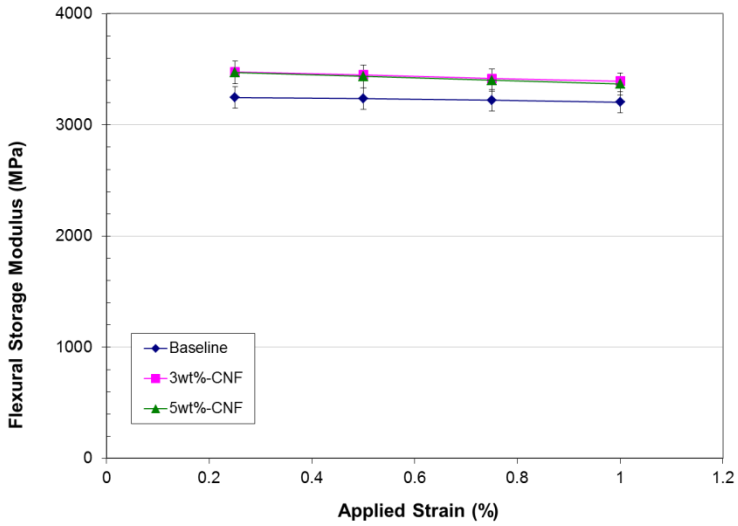


(b)

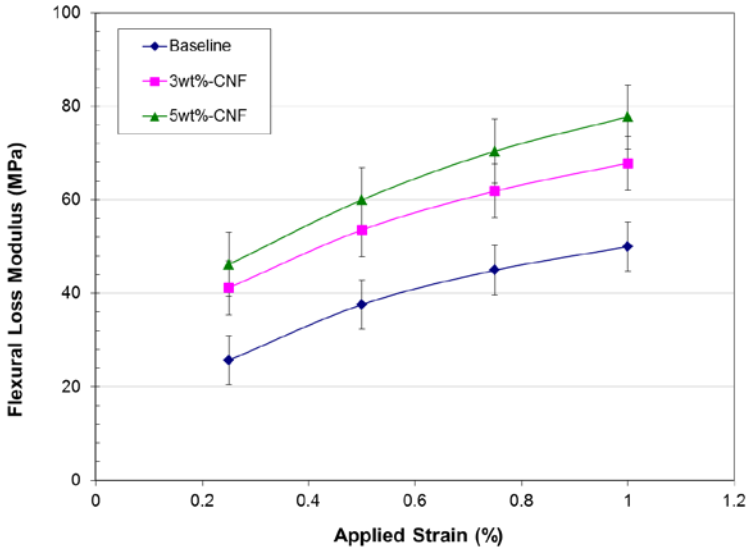

(c)

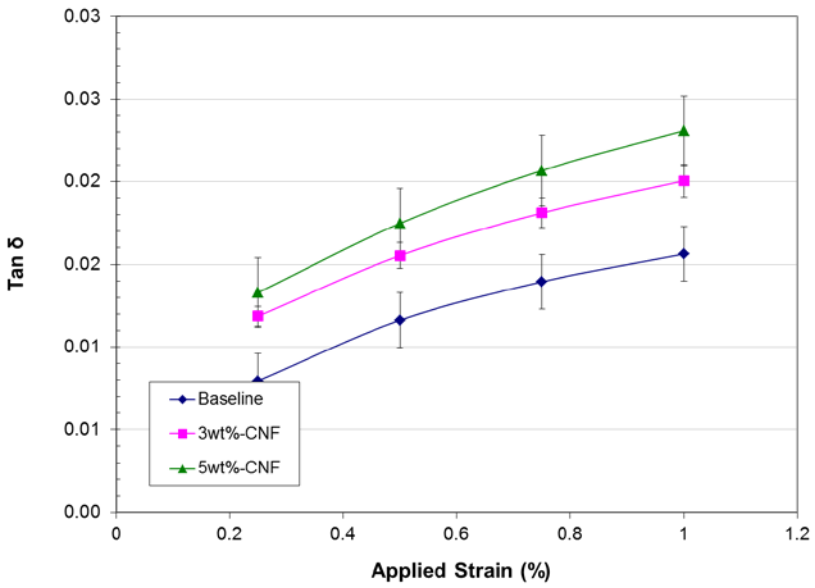


Figure 9: (a) Storage modulus vs. applied strain results of tensile dynamic cyclic testing of 0, 3, and 5wt% CNF included matrix samples, (b) Loss modulus vs. applied strain results of tensile dynamic cyclic testing of 0, 3, and 5wt% CNF included matrix samples, and (c) Loss factor vs. applied strain results of tensile dynamic cyclic testing of 0, 3, and 5wt% CNF included matrix samples. All tests were conducted at room temperature, 25°C, at a test frequency of 1Hz.

Figure 9(c) shows the loss factor of the baseline samples can be improved up to 67% at 1% applied strain by the addition of 5wt% CNF. The loss factor is calculated as the loss modulus over the storage modulus, thus the strain dependent behavior of the loss modulus is also reflected in the loss factor. As well the increasing loss factor with increased filler loading is seen at all investigated strain levels.

## 2.5 Single filler (CNF) modeling – effect of aspect ratio

In initial literature reviews it was found that Finegan, et al.[20] have developed a constitutive damping model for characterizing the damping behavior of filled resins, including nano fillers. This approach is based on short fiber composite theory, coupled with experimental observations to determine fiber orientation distributions. In initial inquiries Finegan's model was implemented exactly as reported and compared to known experimental results to validate this initial model. It was found that the model could accurately predict trends in the damping performance; however it did not accurately predict damping loss factors.

The model reported by Finegan, et al. uses the Halpin-Tsai equations to calculate the components of the stiffness matrix $C_{ij}$ for a unidirectional aligned fiber filed composite as follows:

$$C_{11} = E_{11} = \frac{1 + 2\left(\frac{l}{d}\right)\cdot\eta_L\cdot V_f}{1 - \eta_L\cdot V_f}\cdot E_m \tag{2}$$

$$C_{22} = E_{22} = \frac{1 + 2\left(\frac{l}{d}\right)\cdot\eta_T\cdot V_f}{1 - \eta_T\cdot V_f}\cdot E_m \tag{3}$$

$$C_{12} = C_{66} = E_{12} = E_{66} = \frac{1 + \eta_G\cdot V_f}{1 - \eta_G\cdot V_f}\cdot G_m \tag{4}$$

$$C_{23} = E_{23} = \frac{1 - \xi\cdot\eta_{TS}\cdot V_f}{1 - \eta_{TS}}\cdot G_m \tag{5}$$

Here $V_i$ is the corresponding volume fraction of the constituent denoted by the subscripts f and m, representing fiber and matrix respectively as well l and d represent the fibers length and diameter; and where the constituents of the stiffness matrix coefficients are given as:

$$\eta_L = \frac{\left(\frac{E_f}{E_m}\right) - 1}{\left[\frac{E_f}{E_m} + 2\left(\frac{l}{d}\right)\right]} \qquad \eta_T = \frac{\left(\frac{E_f}{E_m}\right) - 1}{\left(\frac{E_f}{E_m} + 2\right)} \qquad \eta_G = \frac{\left(\frac{G_f}{G_m}\right) - 1}{\frac{G_f}{G_m} + 1}$$

$$\eta_{TS} = \frac{\left(\frac{G_f}{G_m}\right) - 1}{\frac{G_f}{G_m} + \xi} \qquad \xi = \frac{\left(\frac{K_m}{G_m}\right)}{\left(\frac{K_m}{G_m} + 2\right)} \qquad K_m = \frac{E_m}{3\left(1 - 2\nu_m\right)} \tag{6-11}$$

Here the subscripts f and m represent fiber and matrix properties respectively; E, and G are correspondingly elastic and shear moduli respective to the constituent denoted in the subscript. From this basic fiber composite theory it becomes possible to predict the elastic response of the fiber filled composite assuming that the fibers are aligned in the longitudinal direction. Given the nature of short fiber and nano fiber filled

composites it is well known that the fillers are not aligned, and more over it is desirable to have a uniformly random distribution of the fillers. To correct for this, experimental measurements were made to using x-ray diffraction techniques to determine the orientation distribution of the fillers. This probability distribution of fiber orientations is then used as a weighting function and applied to normalize the second and fourth order tensors used to describe the stiffness matrix. The normalized fourth order tensor is then given as:

$$C_{ijkl} = B_1\left(a_{ijkl}\right) + B_2\left(a_{ij}\cdot\delta_{kl} + a_{kl}\cdot\delta ij\right) + B_3\left(a_{ik}\cdot\delta jl + a_{il}\cdot\delta_{jk} + a_{jl}\cdot\delta_{ik} + a_{jk}\cdot\delta_{il}\right) + B_4\left(\delta_{ij}\cdot\delta_{kl}\right) + B_5\left(\delta_{ik}\cdot\delta_{jl} + \delta_{il}\cdot\delta_{jk}\right) \quad (12)$$

Where $a_{ijkl}$, and $a_{ij}$ are given as follows:

$$a_{ij} = \int_0^{2\pi}\int_0^{\pi} p_i(\theta,\phi)\cdot p_j(\theta,\phi)\cdot\psi(\theta)\cdot\sin(\theta)\, d\theta\, d\phi \quad (13)$$

$$a_{ijkl} = \int_0^{2\pi}\int_0^{\pi} p_i(\theta,\phi)\cdot p_j(\theta,\phi)\cdot P_k(\theta,\phi)\cdot p_l(\theta,\phi)\cdot\sin(\theta)\, d\theta\, d\phi \quad (14)$$

The orientations of the fibers are determined in the following $p_i$ constants where θ the angle with respect to the positive 3 direction and φ is the orientation with respect to the positive 1 direction

$$p_1 = \sin(\theta)\cdot\cos(\theta) \qquad p_2 = \sin(\theta)\cdot\sin(\phi) \qquad p_3 = \cos(\theta) \quad (15\text{-}17)$$

Ψ(θ, φ) is the probability distribution function that is then used to normalize the results based on x-ray diffraction measurements of the fiber orientation distribution, however assuming a uniform random distribution as should be the case for well dispersed CNF it them becomes possible to replace Ψ(θ,φ) in the above equations with a random number generator that has a uniform probability distribution from 0 to 2π.

In order to calculate damping the respective elastic moduli are replaced with the corresponding complex modulus, according to the elastic viscoelastic correspondence principle where

$$E=E'+iE'' \quad (18)$$

Here E' is the storage modulus, while E'' is the loss modulus. Using this relationship in the above equation allows for the calculation of the complex stiffness matrix which can then be used to calculate damping as E''/ E' for any given orientation.

Much of the focus of this work was on the effect of the aspect ratio of the fillers;it has been theorized that there exists an optimal (l/d) or fiber aspect ratio which would optimize damping performance. It had been theorized that smaller fiber aspect ratios down to approximately 19 would optimize damping. In the experimental verification 2 types of nano fillers were used. The large fibers were 200-500nm in diameter x 10-40μm in length. These fibers have a nominal aspect ratio of 71. The smaller fibers have a diameter of 80-200nm x 10-40μm in length, resulting in a nominal aspect ratio of 178. Using the above CNF tensile specimens were fabricated at 3wt% loading along with EPON 862 Epoxy resin used as directed with EPIKURE 9552 Curing agent. The CNF's were distributed using a high speed shear mixer, this technique has proven to result in good dispersion of CNF filler, and as well this dispersion was verified using SEM micrographs in order to ensure a uniform random dispersion. The samples were then tested using a DMA technique on a Bose Electro force 3300 to determine damping loss factors. The results can be seen in figure 10.

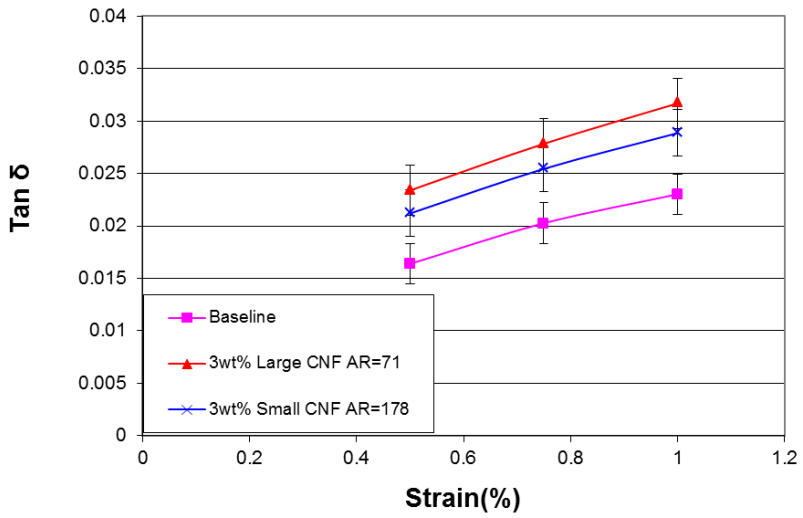


Figure 10: Damping loss factors for baseline and CNF enhanced resin with varying CNF dimensions.

Using the above model the predicted loss factors for the CNF enhanced specimens at 3wt% loading were calculated to be 0.058 for the large CNF and 0.056 for the small CNF. Further investigating the aspect

ratio effect the loss factor was modeled as a function of the aspect ratio, the results of this can be seen in figure 11.

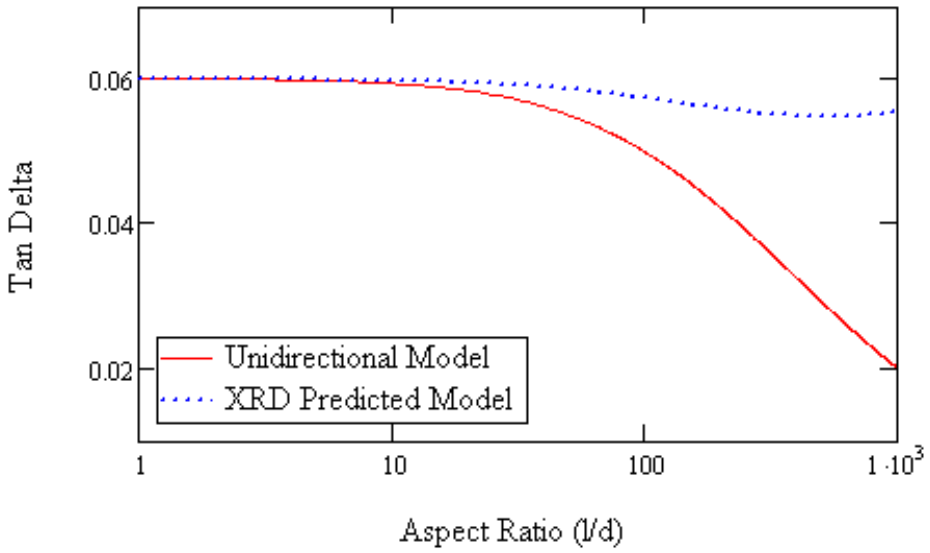


Figure 11: Modeled aspect ratio effect for 3wt% CNF enhanced Epon 862 as compared to the X-ray diffraction experimental results seen in the study from Finnegan et. al.[20]

In looking at figure 10, it is evident that there is a strain dependent behavior associated with the damping enhancement provided by CNF enhancement, while in the model there is no strain dependent behavior as one of the underlying assumptions of the model is that the material is linearly elastic, which is not the case for composites with random distributions of filler. However, as can be seen from the experimental results in figure 10 the smaller CNF having an aspect ratio of 178 exhibit less damping enhancement than the large CNF which have an aspect ratio of 71, suggesting that smaller aspect ratio fillers may be better suited to damping enhancement. Based on the initial research it was determined that damping performance improvements seen in the nano composites translated to improved damping performance in the fiber reinforced composites, however initial modeling, while effective at predicting trends in composite performance was not able to accurately predict nanocomposite performance, as a result additional research was completed to explore the hypothesized issues of the performance discrepancy when the experimental results were compared to analytical predictions, including material properties, filler aspect ratio, and filler

geometry. Given that it has been shown that damping enhancements in the nanocomposite was qualitatively translated to the fiber composite, additional research focused on the development and modeling of nano structured composites, which could later be used as matrix properties in fiber composite modeling.

## 2.6 Damping in fiber composites with nanostructure enhanced resin

Following validation of the damping augmentation resulting from the interfacial frictional sliding, in the nanocomposites, the next phase of the investigation was to utilize the nanocomposite as a nano-enhanced resin to fabricate fiber composites and evaluate the damping properties of an application like composite structure. Beam vibration testing, per ASTM E-756-005, was performed to evaluate the damping enhancement in structural composite panels.

### 2.6.1 Beam Vibration testing results and analysis

Composite panels were fabricated as illustrated in figure 2(b) and beam specimens were cut from the fabricated panels to dimensions of 10mm wide by 270 mm long. Thicknesses for 4, 6, and 8ply composite beams were around 1, 1.5 and 2mm, respectively. Testing was conducted on 4, 6, and 8ply samples. All samples were tabbed 35mm in the clamped end of the beam, using the same construction E-glass fiber composite panel. Response of the beam was measured using a Buel & Kjaar 4517 micro accelerometer, having a mass of 0.800g. The shaker system used was a Vibration Research VR5200. All data collection was made using Vibration Research software, VibrationView 7.0. A schematic of the beam vibration test system is presented in figure 12. Damping analysis was made for the first few resonant flexural vibration modes (< 400Hz); damping loss factors were calculated using the 3dB down method, outlined in ASTM E-756. At least 3 beams of each laminate configuration, 4, 6, and 8ply, were constructed in baseline form (carbon fiber-epoxy composites) as well as 5wt% CNF included carbon fiber-epoxy composites. The tests were run on the beams at maximum input excitation, which is the same order as beam thickness. The beam vibration test began with a frequency sweep from 1 to 400Hz in order to identify fundamental frequencies for the resonant modes. The testing was then transitioned to a piecewise frequency sweep in the vicinity of

each of the resonant modes. The test results are summarized in table 1 and can be seen in figure 13. Figure 13 shows an improvement in the flexural loss factor for the CNF included composites relative to their respective baseline comparators for all samples in the investigated modes. 6ply beams with 5wt% CNF inclusion exhibit substantial increase in loss factor at a given amplitude excitation.

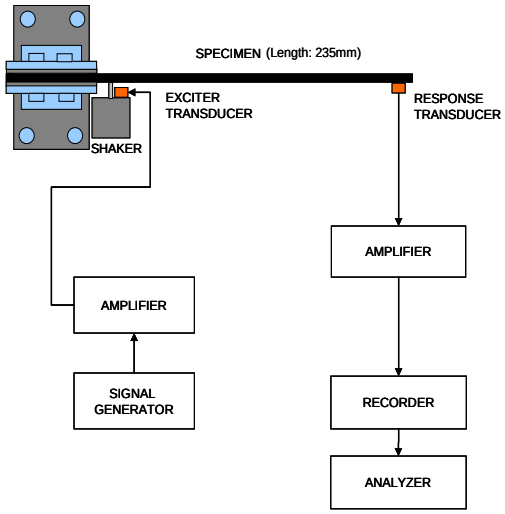


Figure 12: Schematic beam vibration shaker setup, showing the location of shaker input and response measurement

Table 1: Summary of flexural loss factors for frequencies up to 400Hz covering at least the first 2 resonant modes of carbon fiber composite beams tested with shaker at specified frequency ranges and input amplitudes.

| Resonant Mode | I | II | III |
|---|---|---|---|
| Frequency and amplitude | 15-20 Hz @ .7mm | 80-150 Hz @ .2mm | 250-350 Hz @.03mm |
| 4-ply Baseline Loss Factor | 0.05 | 0.03 | 0.017 |
| 4-ply 5wt% CNF Loss Factor | 0.054 | 0.043 | 0.019 |
| Loss Factor % Increase | 8.0 | 43.3 | 11.8 |
| | | | |
| Frequency and amplitude | 15-25 Hz @ .3mm | 130-170 Hz @ .01mm | - |
| 6-ply Baseline Loss Factor | 0.016 | 0.026 | - |
| 6-ply 5wt% CNF Loss Factor | 0.022 | 0.06 | - |
| Loss Factor % Increase | 37.5 | 130.8 | - |
| | | | |
| Frequency and amplitude | 15-25 Hz @ .6mm | 140-200 Hz @ .15mm | - |
| 8-ply Baseline Loss Factor | 0.048 | 0.013 | - |
| 8-ply 5wt% CNF Loss Factor | 0.06 | 0.02 | - |
| Loss Factor % Increase | 25.0 | 53.8 | - |

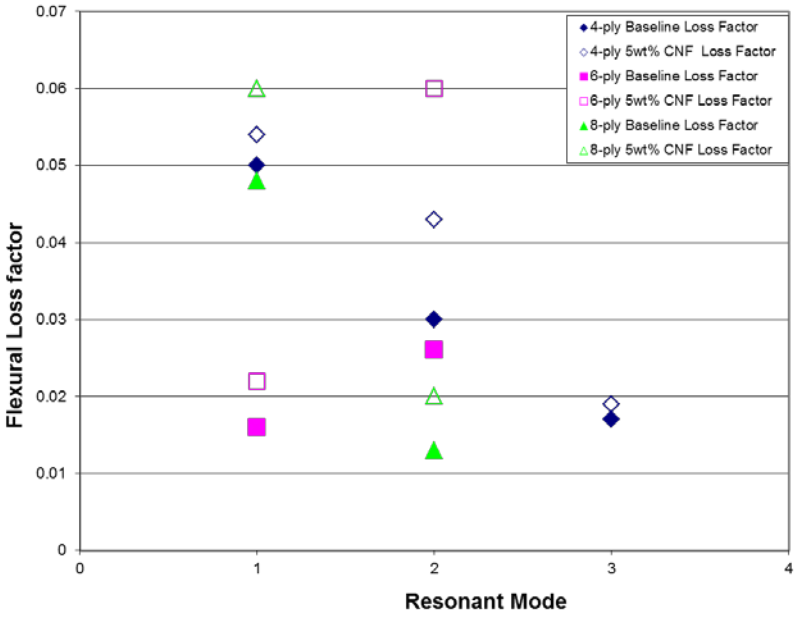


Figure 13: Flexural loss factors for the first 2 or 3 resonant modes for 4, 6, and 8 ply composite beams (Note that the excitation amplitudes for each mode are presented in table 1).

### 2.6.2 Dynamic cyclic testing of fiber composites

In an effort to reduce the intrinsic effect of air drag seen on the beam vibration specimens vibrated in the atmosphere, particularly at mode I resonance, dynamic cyclic testing was used to virtually eliminate the effect of air damping and further investigate the intrinsic strain dependent behavior of the CNF included carbon fiber composite beams, dynamic cyclic testing was performed in tension mode. All dynamic cyclic testing of the fiber reinforced composites were done on 4ply beam specimens with dimension of 42mm long X 6.5mm wide and ~1mm thick. These beam samples were then tabbed 16mm on both ends with material cut from the same composite panel; all sample preparation was conducted according to Gibson[1]. Dynamic cyclic testing was performed at similar initial conditions to those shown in figure 8, with applied strains of .6, .75, .9, and 1%. The applied strain amplitudes were limited to the linear elastic range of the material. Figure 14 shows the resulting loss factor for the 4 ply composite panel specimens. It is clearly seen that there exists a strong strain dependent behavior discovered in the previous investigations of the

polymer composites (CNFs-epoxy composites). The 5wt% CNFs included fiber composite samples show damping enhancement averaging 47% relative to the baseline composite samples at an applied strain of 1% (figure 14). Note that this behavior is fairly consistent with improvements noted during the initial investigation of the baseline (pure epoxy).

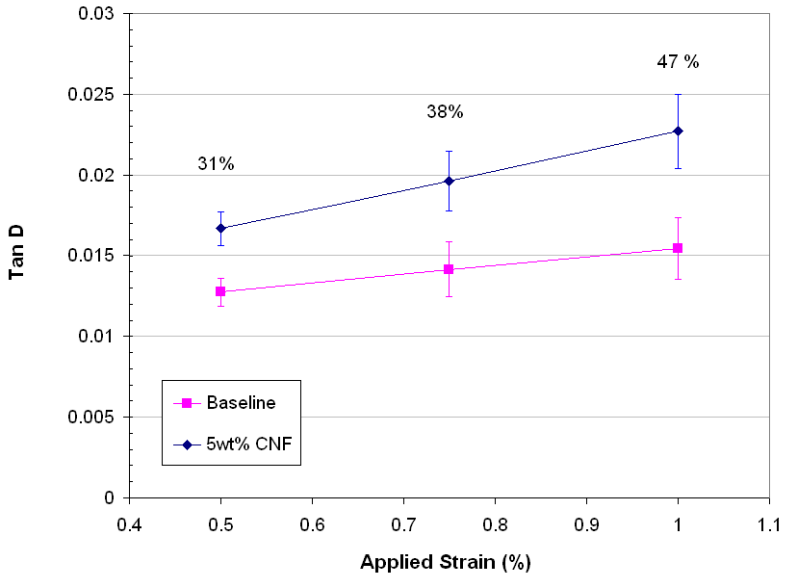


Figure 14: Loss factor vs. applied strain results for 4 ply carbon fiber composite specimens of 0 and 5wt% CNF inclusion. All tests were conducted in tension on a beam specimen 6mm x 40mm gauge length. All tests were run at room temperature, 25°C and at a test frequency of 1Hz.

## 3. Damping in nanostructured composites with multiple fillers

Damping is often one of several requirements in modern composites, a review of the literature indicates that there has been a great deal of effort devoted to engineer specific material performance objectives utilizing nano scale inclusions for everything from damping enhancement, to thermal stability and electrical reistivity[2-19,] Realizing that the next generation of high performance composites utilizing nanoscale fillers to tailor damping performance, will likely utilize other nanoscale fillers to engineer other performance demands, in a multifunction fashion, it becomes increasingly important to understand the damping behavior when more than one filler is used to engineer performance objectives.

## 3.1 Materials and fabrication

In order to obtain experimental data hybrid composites were prepared using two different fillers, CNF and $SiO_2$ particles. The primary (large) CNF were used having a nominal aspect ratio of 71, while the $SiO_2$ particles used where spherical, having a nominal aspect ratio of 1. The technical challenge here is the fabrication of samples with a uniformly dispersed filler loading; as the filler loadings increase, agglomeration of the filler material presents a substantial technical challenge for further manufacturing and fabrication processes. Therefore, fillers and filler loadings were chosen that resulted in substantial enhancements to the baseline epoxy, while still allowing for uniform dispersion by means of high speed shear mixing. Four different types of composites were fabricated varying filler type and loading. Specifically, the CNF was used at 3 wt% for CNF enhanced epoxy. In addition to that the $SiO_2$ particles were varied at 3, 6, and 9 wt%. All of the samples were prepared utilizing the same fabrication method outlined earlier and seen in figure 2(a). Prepared samples had dimensions as seen in figure 3(b), for use with DMA testing. The morphology of the fracture surfaces of the composites was examined with SEM characterization, which confirmed the dispersion quality of hybrid composites prepared through the mechanical direct mixing method. It can be seen in figure 15 that uniform distribution of multiple fillers, at the highest filler loading, 3wt% of CNF and 9wt% of $SiO_2$, was observed.

## 3.2 DMA results and analysis

Dynamic mechanical analysis (DMA) testing was performed to investigate the effect of each of the fillers, both separate and together on the viscoelastic response including damping with respect to temperature. All analysis was done on a Perkin-Elmer diamond lab DMA instrument in flexure. The testing temperatures were varied from -50°C up to 130°C. It should be noted that the upper limit of this temperature range is above the glass transition temperature (Tg) for the neat epoxy (baseline), however this allows Tg of the composites to be clearly identified, providing an indication of the reinforcement effect of the fillers. All testing was done at a test frequency of 1Hz under force control (~9.8mN). Testing was done on at least 3 samples of each type; the results presented here are the best fit single response closest to the average data

set response of those samples. Both storage and loss modulus were measured. The loss factor, tan (δ) was calculated as the loss modulus over the storage modulus.

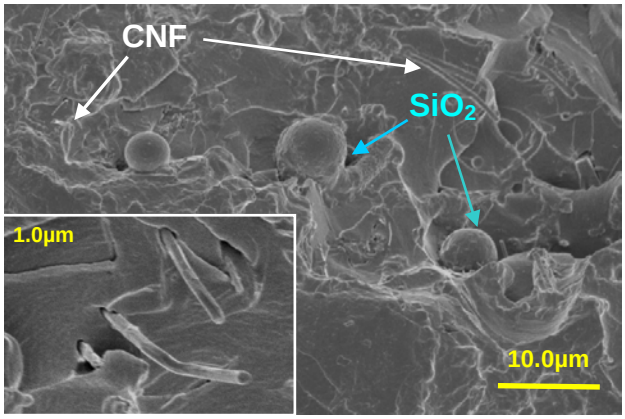


Figure 15: SEM image of fracture surface of 3wt% CNF / 9wt% $SiO_2$ hybrid composite showing uniform dispersion of both fillers.

The effect of filler type was first investigated on mechanical damping by characterizing viscoelastic properties of the polymer composites over given temperature range. It was found that both of the fillers at 3 wt% loadings increased the storage modulus over the entire temperature range tested. At room temperature (25°C), CNF and $SiO_2$ filled composites show a 10% and 5% increase, respectively, in the storage modulus when compared to the baseline epoxy (figure 16). It is expected that CNF had a larger impact on the storage modulus being that it has greater Young's modulus value (~300GPa)[23] than one of $SiO_2$ particles (~76GPa)[22]. The largest storage modulus of the materials was measured from the hybrid composite with 3wt% of each CNF and $SiO_2$ particles (figure 16), showing 18.6% enhancement in storage modulus over the neat epoxy at room temperature. Similar trends were observed in loss modulus responses for the composites (figure 17), in which both of the fillers at 3wt% loading increased the loss modulus values and the largest enhancement was in the hybrid composites with 3wt% of each of the fillers over the temperature range in this study. It can be seen that the addition of $SiO_2$ particles slightly increases the loss modulus (6.3%), while the CNF inclusion at the same loading has a more pronounced effect (31.3%) when

compared to the baseline at room temperature. The improvement of the loss modulus in CNF filled composites over the $SiO_2$ particles filled composites would be attributed to the aspect ratio of the filler[15, 20], much larger interfacial contact area between the filler and matrix[21], and possibly larger stiffness mismatch between filler and matrix[21], which can result in a greater chance of frictional energy dissipation. It is interesting to note that the hybrid composites with 3wt% of each of the two fillers show an increase of ~37.9% in the loss modulus, displaying linear superposition of the improvement in loss modulus from each of the fillers. The damping loss factor, tan (δ) can be obtained from the ratio of the loss modulus to the storage modulus. The greatest loss factor (0.0365) was measured from the composites with 3 wt% of CNF showing more than 20% enhancement in damping over the baseline epoxy with the loss factor of 0.0303 at room temperature, while 3 wt% $SiO_2$ reinforced composites and the hybrid composites with 3 wt% of each of the fillers exhibit 3.6% and 15.8% improvement, respectively in the damping loss factor. It was noticed that the glass transition temperature ($T_g$) is increased as filler material is added to the epoxy. It was observed that the pure epoxy and 3 wt% $SiO_2$ composites have $T_g$'s of 91°C and 92°C, respectively, while 3 wt% CNF filled composites and the hybrid composites have 93.4°C and 94°C, respectively. This indicates that the shift in Tg is proportional to the increase in storage modulus for the composites confirming that the nano-filled or micron size particle filled composites are reinforced from the fillers respectively. The DMA data shows that the addition of both fillers to epoxy can improve the reinforcement as well as mechanical damping without any noticeable compromise over the temperature range (-50~130°C) investigated. Additionally, it indicates that the relatively large aspect ratio CNF is much more effective at not only improving the storage modulus but also augmenting mechanical damping when compared with the $SiO_2$ filler having a nominal aspect ratio of 1.

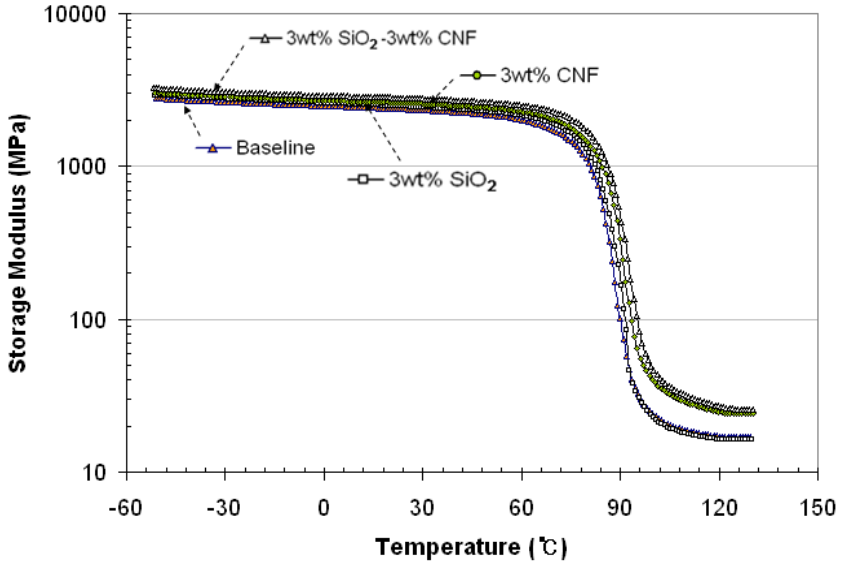


Figure 16: flexural storage modulus vs. temperature for each filler at 3wt% loading.

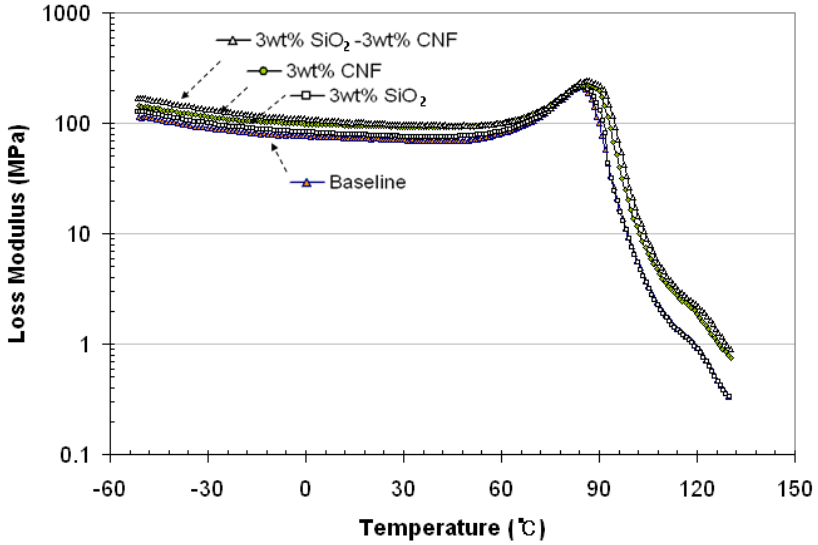


Figure 17: flexural loss modulus vs. temperature for each filler at 3wt% loading.

## 3.3 Multiple filler phase modeling

Realizing the growing importance of understanding the damping behavior of composites with more than one filler phase, it becomes necessary to develop a viscoelastic model capable of dealing with more than one filler phase in the nanocomposite. As well, the use of multiple fillers allows for a simultaneous

investigation of both filler aspect ratio and filler structural properties. To do this the original model presented by Finegan, et al[20], was expanded to account for two filler phases, where the filler phases were separated in to $V_{f1}$ and a $V_{f2}$ respectively to account for both the CNF filler phase and the $SiO_2$ filler phase. Required for this model is a complex modulus for each of the constituents. This analytical investigation focused on the viscoelastic behavior of the composites at room temperature. The properties used for the epoxy matrix were taken directly from the previous DMA data on the baseline epoxy, with a value of $E^*_m$ = 2.23 +*i*0.076 GPa (figure 6). Since the material properties of nano-scale fillers presented a great challenge in measuring them, these properties were estimated based on a literature survey[13,15,21-23] , and taken as follows: CNF, $E^*_{CNF} = 250 + i1.5$ GPa. The $SiO_2$ data found in literature[21] was based on experimental deduction, where a complex modulus for $SiO_2$ powder was found to be, $E^*_{SiO2} = 28 + i0.028$ GPa. Using these material properties the expanded viscoelastic model, equations (12)-(14) was run for desirable loadings of the respective fillers in order to generate the analytical modeling results, and the modeling results were compared with the corresponding test data (figures 18 and 19). In the semi-empirical model the same equations were used, (12)-(14), however the input material properties of the matrix phase was taken as the experimental results of the 3wt% CNF nanocomposite, with a 3wt% filler of $SiO_2$ particles.

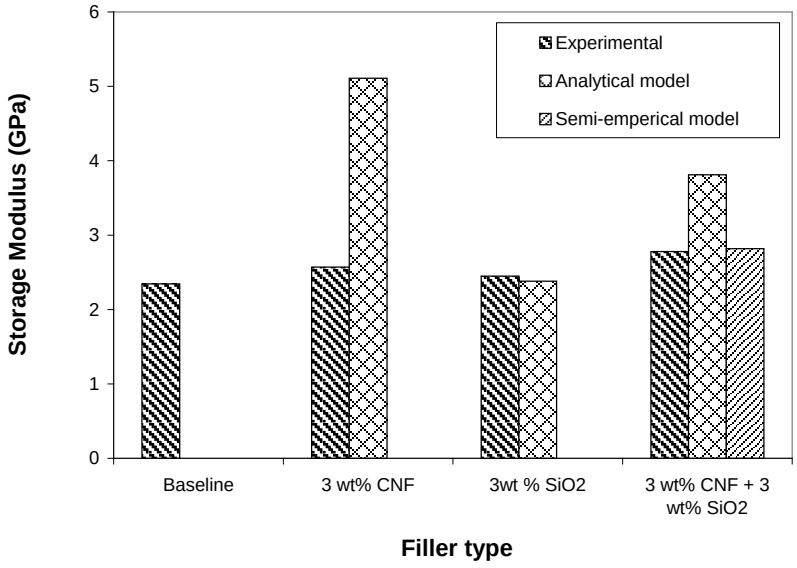


Figure 18: Comparison of analytical and experimental values for storage moduli of composites with respect to filler type

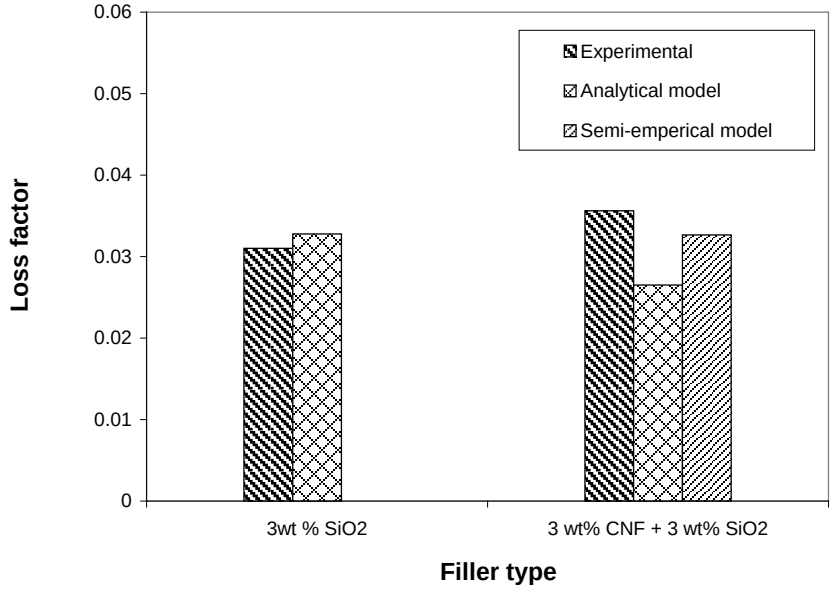


Figure 19: Comparison of analytical and experimental values for loss factor of 3 wt% $SiO_2$ particles reinforced composites and hybrid composites with 3 wt% of CNF and 3 wt% of $SiO_2$ particles.

It was observed that the analytical model significantly overestimates storage and loss modulus for the 3 wt% of CNF filled composites. As seen in figure 18, the modeling data of the storage modulus of the 3wt % CNF composites was estimated nearly twice as much as the experimental data, leading to a conclusion that the effective reinforcement provided by the CNF filler may be much smaller than otherwise predicted by constituent properties alone. It also predicted 17.5% less than the measurement in damping loss factor (figure 19). In a sharp contrast, there is very good agreement in viscoelastic behavior between the modeling and test data for the micron size $SiO_2$ nanocomposite, showing only 2.8% and 5.6% difference in storage modulus (figure 18) and loss factor (figure 19), respectively. This would most likely be attributed to the lack of accurate information for the complex moduli of the CNF filler phase as well as assumption of their perfect cylindrical geometry, and uniformly random orientation in the matrix. In fact, it was reported that the reinforcement effect of carbon nanotubes as fillers with a high aspect ratio can be significantly reduced due to their waviness when embedded in polymer matrix[23-25]. Correspondingly, the hybrid composites with the CNF and $SiO_2$ fillers were also substantially overestimated for the storage and loss modulus with the analytical model. In order to avoid this considerable overestimation when the properties are analytically

predicted, a semi-empirical model for the hybrid composites with multiple filler phases was developed. The empirical data was used along with a two phase version of the viscoelastic model where the matrix and the filler were taken to be 3 wt% of CNF filled epoxy and the $SiO_2$ particles, respectively. The viscoelastic responses of the hybrid composites with both the fillers were estimated with the semi-empirical model. The modeling results are compared with the DMA data, and the modeling data with the expanded three phase analytical model (figures 18 and 19). It can be seen that the semi-empirical model estimates by only 1.3% greater and 8.29% less in storage modulus and loss factor, respectively when compared with the measured data of the hybrid composites, while the three phase analytical model substantially overestimates the storage modulus around 37% greater and underestimates the loss factor by 25.5%. Based on these results, it indicates that disparity between modeled and experimental results may well be a direct result of the higher aspect ratio filler, specifically CNF in the this case. It has been shown that the non-cylindrical nature, or waviness of the filler observed in SEM images contributes to a greatly reduced effective reinforcement in the nanocomposite when compared to the theoretical perfect cylinder[24]. Additional modeling work is later proposed to address waviness in a complete viscoelastic response model.

## 4. Effect of filler geometry and orientation on the damping response in nanostructured composites

This area of research has been devised to look at the large performance gaps of nanostructured composites, relative to analytical modeling thereof, where modeling tends to drastically overstate the performance of nanocomposites. In reviewing the literature there have been a number of works that reported on the use and modeling of high aspect ratio fillers such as CNT and CNF for the express purpose of tailoring the viscoelastic response of nanocomposites. However, there is currently a large gap in performance of nanocomposites, where in the current analysis techniques tend to overstate the performance achieved relative to experimental results. This discrepancy has been attributed to a number of factors ranging from non-perfect geometry, to issues at the interface between matrix and filler. However, there has not yet been a detailed investigation of the ability to accurately predict composite viscoelastic characteristics based on constituent properties. One of the most common approaches to modeling high aspect ratio nano fillers is to

assume a perfect cylindrical geometry, even though it is well reported that these fillers can have a significant curvature or waviness to them[24]. Similarly, many published models are two dimensional, although high aspect ratio nanofillers are by nature randomly oriented in all three dimensions. Additionally, the constituent material properties for the nano scale constituents present a large challenge in light of conventional analysis and modeling techniques, as it is nearly impossible to measure the material properties of the fillers by conventional testing means, due to the size scale of the materials. Utilizing experimental results, coupled with strain energy techniques and finite element analysis (FEA) results, this study looks at the effect of random filler orientation and filler waviness on the effective filler loss factor which is calculated through the techniques used.

It has been shown in the previous investigation presented and elsewhere in the literature[1-4,20,24] that the inclusion of a small fraction of high aspect ratio nanofillers can serve to improve the damping capacity of nanostructured composites. Studies to this point have indicated a strong strain dependent response in the total damping capacity of the nanostructured composites utilizing CNF to augment damping capacity. This is due, in part, to the random distribution of filler orientations seen in the nanocomposites. The random distribution of filler orientations is thereby relative to the load applied to the composite that results in a critical shear stress thresholds being surpassed, at the nano scale, allowing the filler to slip relative to the matrix, resulting in frictional energy dissipation as heat and thereby inducing damping to the high aspect ratio filler nanocomposite. This non-linear behavior of the total damping performance is well understood, as are the strain energy methods used here, hence all modeling was done at low amplitude strain, presumably before frictional sliding takes place, keeping all modeling in the linear elastic range in an effort to better understand the intrinsic material performance. While the intrinsic loss factor of CNF is not necessarily substantially higher than that of the polymer the increased damping has been at least partially attributed to a nanoscale slip between the filler and the matrix. This nano scale slip can then dissipate energy as heat, once the load is removed the van der Waals bonds that were broken to allow the slip are then reestablished, which allows for a localized recoverable nanoscale failure that can add damping capacity to a nanocomposite. The key to this type of damping is the use of high aspect ratio fillers such as nano tubes or nano fibers, the geometry of high aspect ratio fillers allows for a shear stress buildup at the

ends of the fiber, with load, once a critical shear stress level is achieved de-bonding occurs and filler is allowed to slip relative to the matrix. The load required to generate this critical shear stress, which allows for slip, is relative to both the filler orientation as well as the loading direction, therefore, the random orientation of fillers seen in most nanocomposites leads to a strain dependent response in the viscoelastic characteristics of the composite. In looking at nanostructured composites utilizing high aspect ratio fillers there is limited to no control of the filler orientation in bulk composite materials. Some manufacturing techniques can impart a range of preferential filler orientations, however, in most cases there is essentially a random distribution of filler orientations. The random distribution of filler orientations in conjunction with the fact that the orientation relative to the loading direction determines the amount of load required to allow for slip, is the basis for the strain dependent response seen in the viscoelastic properties measurements on nanocomposites. As the strain levels increase with increasing load, an increasing fraction of the nanofiller reaches a critical shear stress which allows for slip that can dissipate energy and improve damping capacity. The use of high aspect ratio fillers to augment the viscoelastic performance of the composites has shown great promise for use in many applications, particularly in aerospace applications where use of composite materials is rapidly expanding, but currently in need of damping and noise attenuation capabilities in composite materials. Currently, the limiting factor preventing application uses of this technology involves a complete fundamental understanding of both the materials and mechanisms that would allow for detailed modeling to accurately predict composite performance, both in structural and viscoelastic performance. A key factor in the ability to accurately predict composite performance is a complete understanding of constituent material properties in nanocomposites. This is one of the largest challenges and the size scale of the fillers prevents conventional material testing methods from being used to characterize constituent properties. This fact has led to the use of in situ measurements of nanocomposites in order to attempt to back out constituent intrinsic properties. The focus of this study was a fundamental investigation of the effects of both filler orientation and waviness, however the techniques used here coupled with an experimental investigation were also used to back out the effective filler loss factor, which is detailed later. In the investigation of filler waviness it was discovered that a small amount of filler waviness may actually enhance the load transfer capabilities to the filler, thus enhancing the overall structural performance of the

composite. This finding is different from earlier investigations that conclude any amount of waviness adversely affects the structural performance of the composite[26-29], however other studies have concluded that curvature of the filler may serve to increase the interfacial stress transfer abilities of the composite[30], and may offer additional insight to the fundamental mechanisms at work. In the comprehensive approach detailed below, utilizing experimental as well as analytical and modeling tools, we see the profound effect that filler geometry and overall composite structure can have on the performance of nano structured composites.

## 4.1 Materials and Composite Fabrication

In order to fabricate the composites, EPON™ Resin 862 purchased from Miller Stephenson Inc. was used as the polymer matrix with curing agent (EPIKURE™ 9553) at a weight ratio of 100:16.84. Graphitized CNFs with dimensions of 200~500 nm in diameter and 10~40 μm in length from Nano Amorphous Materials Inc., were selected for the filler material. CNF filler was used as received, without any functionalized additional bonding so as to investigate the best potential for slip at the filler matrix interface. For fabrication of the composites, the filler was then added at appropriate amounts to reach desired loading (3wt%, and dispersed with a high speed mechanical shear mixer (Speed Mixer DAC150 FV-K). Upon completion of the resin preparation the epoxy resin was poured into molds and cured at room temperature for 24 hr. All of the samples prepared had dimensions of 20 mm in length, 10 mm in width, and 2mm in thickness. Testing was done on at least 3 samples of each, neat epoxy and 3wt% CNF composites, and the results presented are the average responses of those samples. This manufacturing process is clearly outlined in figure 2.

## 4.2 Viscoelastic characterization

In this study, dynamic mechanical analysis (DMA) testing was performed to investigate the effect of CNF on the viscoelastic response including damping with respect to temperature. All analysis was done on a DMA (TA instrument-DMA Q800) with flexural mode. The testing temperatures were varied from room

temperature to 120 °C. Note that the upper limit of this temperature range is above the glass transition temperature ($T_g$, 90 °C ) which was measured by DSC (TA instrument- DSC Q20) for the neat epoxy, it allows $T_g$ of the composites to be clearly identified, providing an indication of the reinforcement effect of the CNF. All testing was done at a test frequency of 1 Hz under 1% applied strain with 3°C/min heating rate on single cantilever clamp condition.

## 4.3 Experimental results

The effect of CNF on the viscoelastic response of the polymer nanocomposites was characterized over the given temperature range. It was found that storage modulus over the entire temperature range increased, while the loss factor only increased below $T_g$. At room temperature (25 °C), the storage modulus (3,142MPa) of CNF filled composites show a 12% increase, when compared to the neat epoxy (2,804 MPa) in figure 20. It is expected that CNF had a larger impact on the storage modulus being that it has a greater Young's modulus value (330 GPa), the damping loss factor, tan (δ) can be obtained from the ratio of the loss modulus to the storage modulus. CNFs also are activated in the frictional slip mechanism that generates mechanical damping due to stick slip nature of the damping. The loss factor (0.0336) was measured from the composites with 3 wt% of CNF showing more than 16% enhancement in damping over the neat epoxy with the loss factor of 0.0289 at room temperature. The loss factor of neat epoxy is greatly affected by the operating temperature. This loss factor varies with increasing temperature and achieves a maximum value corresponding to the $T_g$ because of the intrinsic matrix viscoelasticity[31].

Importantly, the $T_g$ is increased as filler material is added to the neat epoxy. It was observed that the neat epoxy and 3 wt% of CNF filled composites have $T_g$ of 90 °C and 91.1 °C, respectively. Apparently, the shift in $T_g$ is shown to be proportional to the increase in storage modulus for the composites, confirming that the CNF-filled nanocomposite is reinforced by the filler accordingly. Note that the experimental errors stayed within 2.4% of the mean values.

(a)

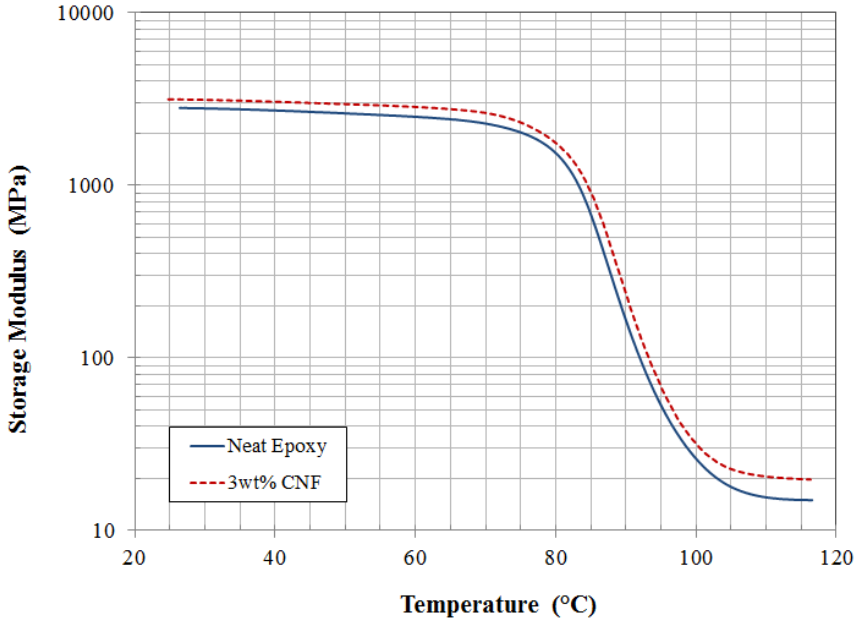


(b)

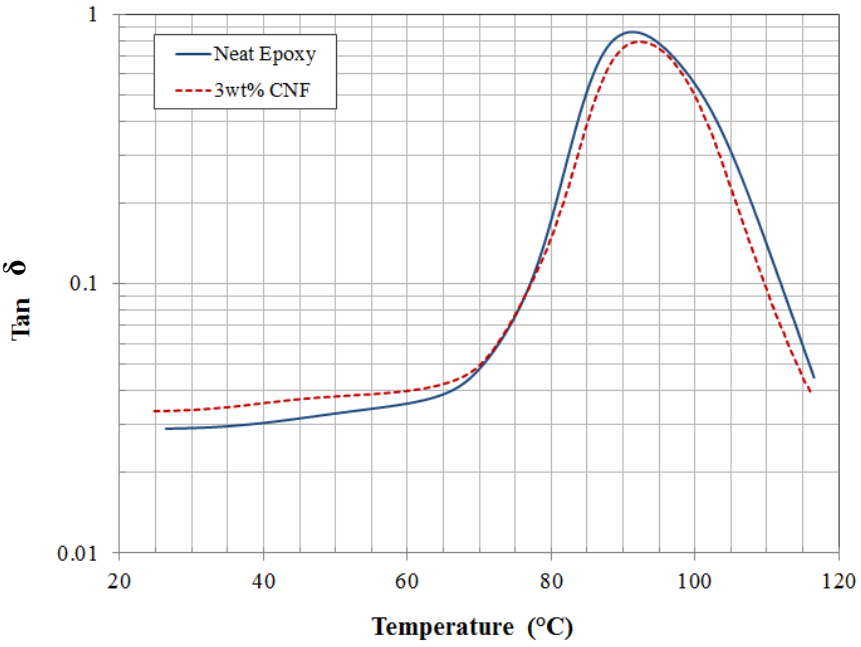


**Figure 20:** (a) Storage modulus vs. temperature for CNF filler at 3 wt% loading, (b) Tan Delta vs. temperature for CNF filler at 3 wt% loading.

## 4.4 Finite element analysis

In the literature there has been some reported work on modeling the effect of nanofiller waviness, as well there has been some work on the effect of filler orientation in nanocomposites, however these works are all related to the structural reinforcement of the nanocomposites. However, there remains a fundamental lack of understanding of the viscoelastic response of the nanocomposites, which manifests an area of growing interest. Previous modeling work, examining the stiffness/strength response, has employed a variety of techniques ranging from modeling the bulk composites as a representative volume element (RVE) of periodically aligned short fibers[31], to modeling the structural properties of a single wavy filler embedded in epoxy[26,30,33,34]. Additionally, the effects of different matrix properties have been investigated including the effect of a hyperplastic, rubbery matrix[35]. As well, pull out modeling has been used to better understand the interfacial properties of wavy high aspect ratio nano filled composites[30]. Yet, there has been little effort utilizing these techniques to understand the viscoelastic response of these high aspect ratio nanocomposites, which have been widely researched experimentally for the induced damping capacity achieved in their use. To gain insight in to the effect of filler orientation and waviness, on the viscoelastic response, of nanocomposites utilizing high aspect ratio fillers, finite element analysis (FEA) models of a single filler in epoxy were developed using ANSYS in both 2 and 3 dimensional modeling. In all models the filler was modeled to have dimensions of 35nm in diameter by 25μm long, consistent with the filler geometry of the filler used to generate the experimental results, and the matrix was modeled as a 50μm square, or cube, respectively, with the filler centered in the matrix block. This geometry results in filler loading of 3 wt% in our modeling; this was chosen due to the ability to accurately model single fillers and avoid matrix geometry changes as well as edge effects in all the model results presented. For comparisons to experimental work, additional models using the same properties were used with varying matrix geometries to generate representative models of 3 wt% filler loadings free of edge effects. All matrix properties were modeled having a Young's modulus of 3GPa as determined by experimental work and Poisson's ratio of 0.3 as reported previously[1]. All CNF fillers were modeled to have material properties of 330 GPa and 0.3 Poisson's ratio as taken at adjusted effective values based on modeling work developed in chapter 3. To investigate the effect of filler orientation relative to the loading direction a series of 2 dimensional models

were initially developed having nominal filler orientations, with respect to loading direction, of 0° to 90° in 10°increments, noting the symmetry of the model about 90°. To investigate the effect of filler waviness models were created with filler waviness factors of 0 to 0.5 in 0.05 steps. Filler waviness is defined as the amplitude of the curvature of the filler (a) divided by the filler length (L) as measured along the arc length of the filler, a filler waviness of 0 would be perfectly straight filler, while a filler waviness of 0.5 would be a filler doubled over on itself, this can be seen depicted in figure 21. For the 2D models developed in ANSYS a solid 182 element type was used. Boundary conditions were applied with the use of a multi-point constraint such that the unconstrained edges move parallel to their original orientation, allowing for scalability and chaining of the representative volume elements. A 1% tension strain was applied to the model and the FEA program was used to calculate the strain energy in each element of the model for prediction of the effective loss factor. This load condition is same as DMA experimental conditions since the stress and strain at the RVE level is either tension or compression in the flexural DMA mode. The use of the strain energy distribution in calculation of the loss factor will be explained in the next section. Looking at a representative 2D model, seen in figure 22, the left edge would be constrained in the X direction, the lower edge would be constrained in the Y direction and the right edge would be displaced in the X direction a distance required to reach the desired strain level. In modeling the 3D representation of the system it was found that there was a negligible difference in the 2D and 3D results, so for efficiency and convenience, 2D results are presented throughout this study.

(a) (b)

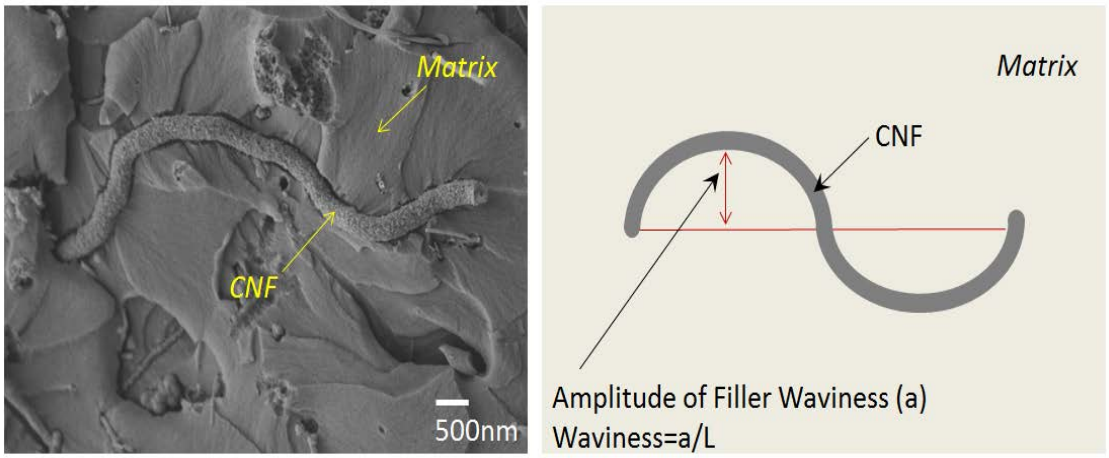


**Figure 21:** (a) Representative SEM image of CNF waviness on fracture surface of CNF filled nanocomposite (b) Schematics of filler waviness where the amplitude of the filler waviness, defined as (a) is divided by the axial length of the filler (L) to obtain a waviness factor.

(a) (b)

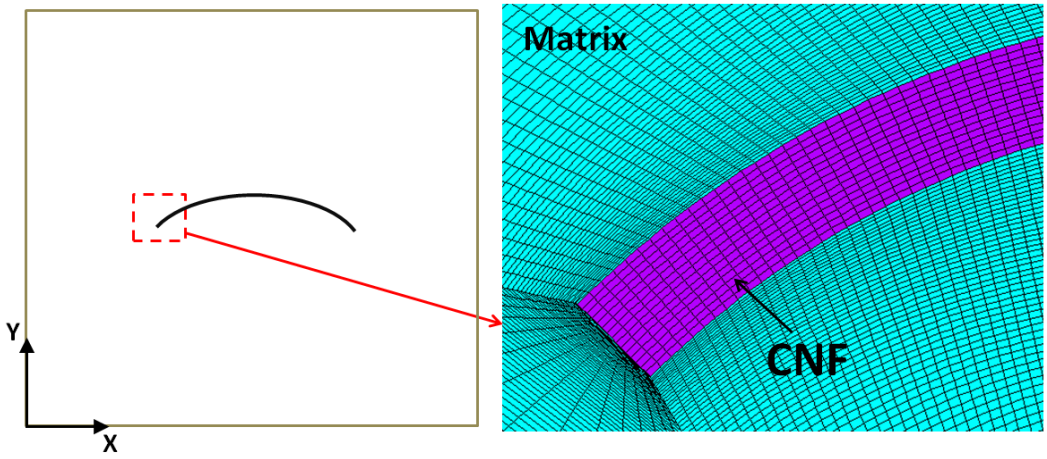


**Figure 22:** (a) Schematic for RVE and (b) Meshed FEA model.

## 4.5 Strain energy methods

It would be desirable to directly characterize the intrinsic loss factor of the filler phase. However given the challenges in measuring the intrinsic properties of the nano scale fillers, especially high aspect ratio fillers such as carbon nanotubes or carbon nanofibers, the concept of the effective loss factor is used in this study by employing the strain energy method in conjunction with FEA modeling. It will be still beneficial to understand and gain fundamental insight in to the effect of the intrinsic characteristics of the high aspect ratio fillers on the viscoelastic response of such nanocomposites. Strain energy methods are well documented in the literature[1] for analyzing viscoelastic properties. The strain energy methods state that the total damping provided by a given constituent in a composite is equal to the fraction of the total strain energy stored in the constituent multiplied by the intrinsic loss factor for that given constituent, and the total loss factor of the composite is then the sum of the constituent loss factors multiplied by the fractional strain energy stored in each respective constituent, and this is stated formally in equation (19), where n is defined as the total number of constituents, $\eta_i$ is defined as the constituent loss factor, $U_i$ is the total strain energy stored in the $i^{th}$ constituent, and $U_{total}$ is the total strain energy in the composite[36].

$$\eta_{composite} = \sum_{i}^{n} \eta_i \frac{U_i}{U_{total}} \tag{19}$$

The modeling developed here utilizes only two constituents, the CNF filler and the epoxy matrix. Utilizing FEA to characterize the fractional strain energy stored in each constituent of the composite allows for evaluation of the effective loss factor of the filler in a nanocomposite. The contribution of the filler towards the composite loss factor being proportional to the fractional strain energy stored in the filler phase of the composite, this study investigates the fractional strain energy stored in the filler phase of the composite as function of both filler orientation and waviness in order to gain insight to the effect these two factors can have on the overall viscoelastic performance of the composite. From a practical application stand point these techniques can be utilized in conjunction with experimental observations to back out effective filler loss factors. Using FEA models to calculate the fractional strain energy stored in each

constituent of a representative volume element of the composite and assuming that the matrix loss factor is known from DMA tests of the neat epoxy leaves the only unknown in equation (19) to be the effective loss factor of the filler phase.

In order to investigate the intrinsic loss factor of the filler, FEA was performed to calculate the strain energy stored in each constituent at the aforementioned nominal filler orientations. The intrinsic loss factor of the matrix, in this case EPON 862, was obtained through DMA characterization on the neat epoxy. Young's modulus for the matrix was taken from previous studies in chapter 2, which was input in to the FEA models in order to calculate the strain energy. The storage modulus and the loss factor of a 3 wt% CNF filled composite was measured through the DMA characterization as well. The elastic modulus of the filler was taken as 330 GPa, based on previously presented modeling studies the effect of waviness on the reinforcement provided by wavy filler at a waviness factor of 0.25. This leaves the only unknown in the strain energy equation to be the CNF loss factor, which could then be solved for.

## 4.6 Results and analysis

Figure 23 shows a strain energy density plot of the RVE FEA model with a single CNF filler having a waviness of 0.05 at 1% strain. Here it can be clearly seen that the lowest strain energy density exists in the vicinity of the filler, however the largest Von Mises stress occurs in the filler at a location where the orientation is parallel to the loading direction which can be seen in figure 5. Looking at figure 24 the central portion of the fiber exhibiting the largest stress concentrations seen in the model differs from that of a straight filler in figure 25, where the largest stress concentrations are seen at the filler ends, this key fact is the basis for the fact that a slight curvature may actually serve to enhance the load transfer capabilities of the composite to the filler and may serve to enhance the structural properties of the nanocomposites.

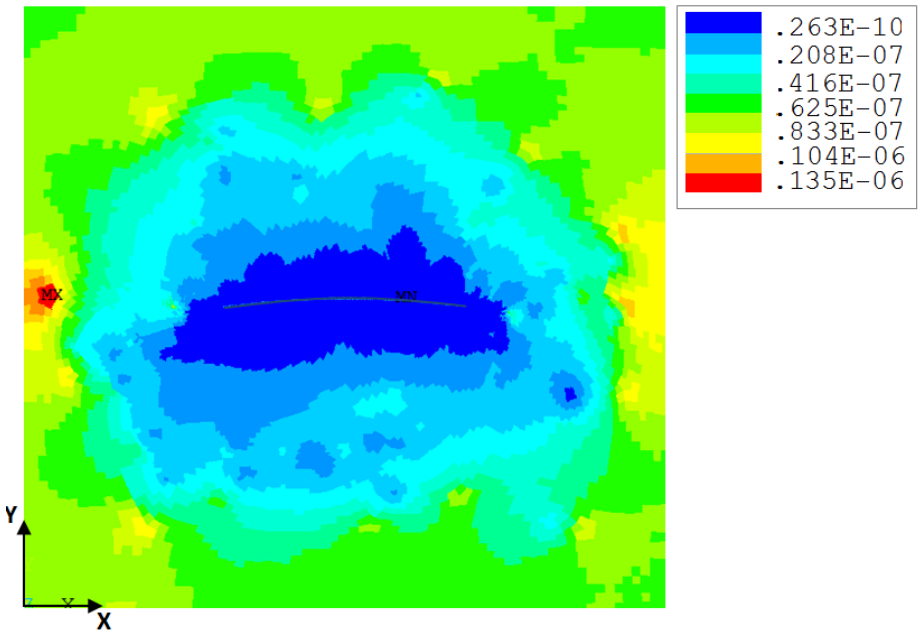


**Figure 23**: Strain energy density (Nm) of model presented in figure 22with a 1% strain applied load.

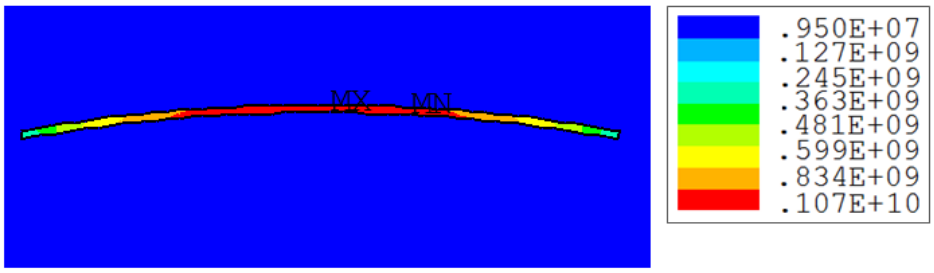


**Figure 24**: Von Mises stress distribution in the vicinity of the filler for model presented in figure 23 with a 1% strain applied load (Pa).

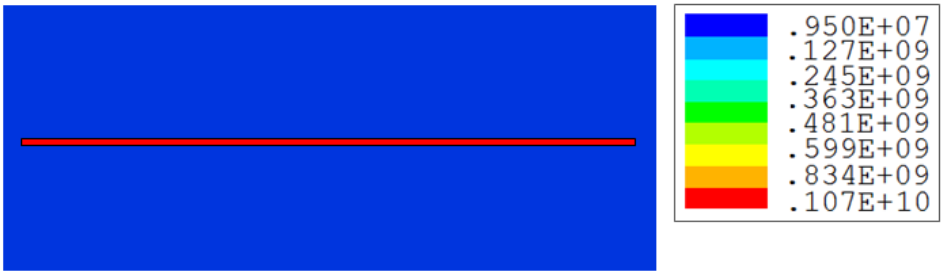


**Figure 25**: Von Mises stress distribution in the vicinity of the straight filler with a 1% strain applied load (Pa).

Figure 26 shows the fraction of the strain energy stored in the filler, as a function of the nominal filler orientation, where the nominal filler orientation is taken as the angle between the loading direction and a straight line connecting the ends of the nano filler. At 0 waviness, representative of a straight filler, it can be seen that the fraction of the strain energy stored in the filler varies inversely to the angle between the filler and the loading direction up to 60°. In the angle range from 60° to 90°, the strain energy in the filler is slightly increasing, which could be attributed to the activation of the matrix Poisson's ratio at large angles relative to the loading direction . It can clearly be seen that the matrix in this case, Epon 862, is much more compliant than the filler, therefore the matrix deformations are substantially larger and thus the strain energies are proportionally larger in the matrix as compared to the filler, particularly at the ends of the filler where large shear gradients are expected at the ends of the filler due to the stiffness mismatch of the matrix and filler. However, the reinforcement effect of the filler can also be seen in figure 24, showing the largest stress occurs in the much stiffer filler phase of the composite. figure 26 shows a variation of 2.2% in the fractional strain energy stored in the filler phase of the composite, relative to the filler orientation. Even with relatively small loading fractions of nano fillers, which is seen in most nanocomposites, this can translate in to large variations in predicted viscoelastic performance of the nanocomposites relative to the calculated effective filler loss factor, given the relatively small strain energy stored in the filler, and therefore underscored the need to evaluate the underlying material characteristics in developing a model. Figure 27 shows the fractional strain energy stored in the filler as a function of filler waviness, at a 0° orientation, where it can be seen that there exists a slight increase in the strain energy stored in the filler at low amplitude waviness while as waviness increases beyond 0.1 there exists a notable decrease in the strain energy stored in the filler. Overall, there is a 1% variation in the fractional strain energy stored in the composites, relative to the filler waviness, which as discussed earlier can have a large implication in the overall predicted performance. In looking at the modeling results in detail the inflection in the low amplitude may be attributed to the fact that a slight curvature to the filler, while still nominally being oriented in the loading direction, can actually serve to increase the load transfer to the filler, this would serve to enhance the structural properties. The key here is that while the goal is to investigate the intrinsic loss factor of the CNF filler, there are a number of factors which play in to the investigation, one of these

being orientation of the filler relative to the loading direction. The intrinsic properties of the nanofiller will not change, however the effective properties of the filler can vary to a large degree based on orientation, though most often taken to have a theoretically random distribution of filler orientations, any preferential orientation achieved in the manufacturing process could serve to dramatically alter the material properties including damping properties. The behavior witnessed as a function of filler orientation and waviness provides some insight to the behavior of the randomly distributed filler orientations seen in nanocomposites with high aspect ratio nano-sized fillers and provides a basis to continue this work expanding the modeling techniques used to get a more realistic intrinsic loss factor for the filler while at the same time characterizing the loss attributed to frictional slip at the interphase accounting for the interphase region.

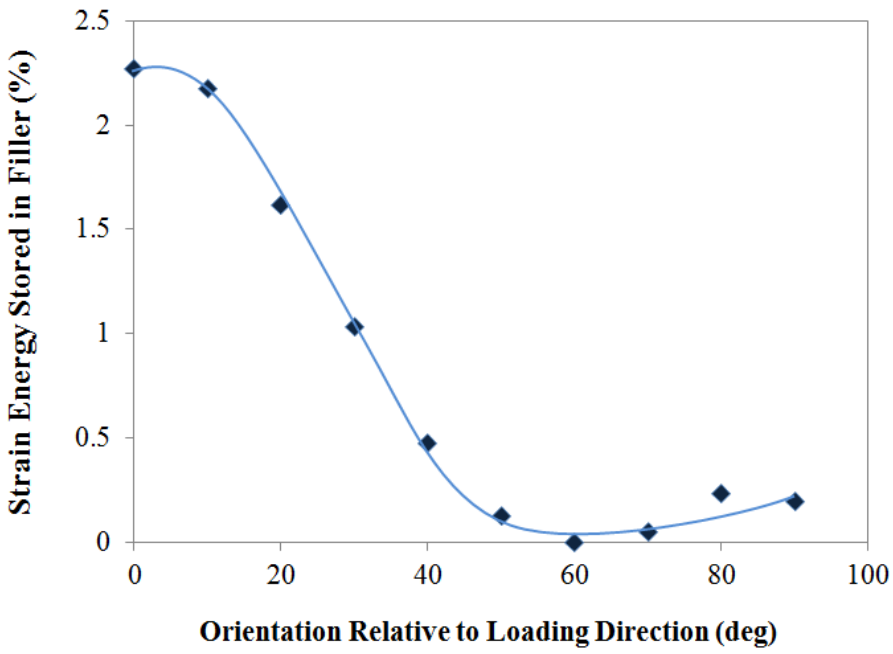


**Figure 26:** Fraction of strain energy stored in the filler as a function of filler orientation.

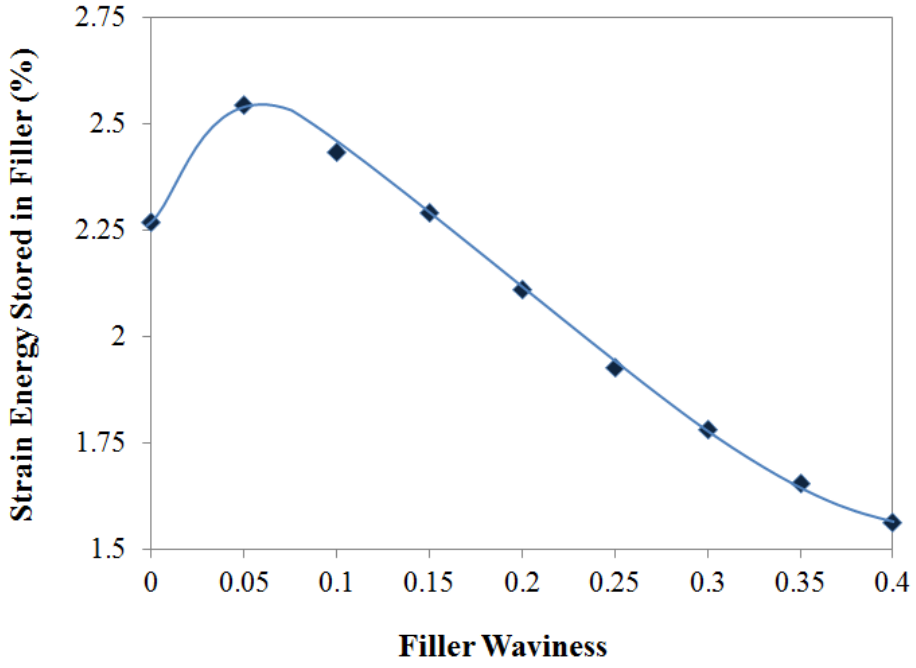


**Figure 27:** Fraction of strain energy stored in the filler as a function of filler waviness.

Figures 28 and 29 show the calculated composite loss factor for a 3wt% CNF filled composite, as calculated by using strain energy methods coupled with FEA, and various assumed filler loss factors in order to look at the sensitivity of the filler loss factor in conjunction with effect of filler orientation and waviness on the predicted viscoelastic performance of the nano filled composite. Both the orientation and waviness factors have large impacts on the calculated composite loss factor, in this particular case there are discrepancies of up to 25%, when compared to the experimental results, in the viscoelastic performance predicted in the composite. In an attempt to gain insight to the effect of both orientation waviness effects on the calculated material performance of the CNF filled nanocomposites we utilized experimental DMA data for 3 wt% CNF enhanced epoxy composites from the experimental work reported above and calculated the effective filler loss modulus by utilizing a representative FEA model (3wt% representation) and the strain energy techniques described above to yield an effective filler loss factor of 0.53. This value was obtained by utilizing a filler waviness factor of 0.2 and averaging the fractional strain energy stored in the filler across all possible orientations to simulate random orientation, as can be seen in equation (20), where

$\eta_{composite}$ is the loss factor for the composite as measured in the experimental study, $\eta_{matrix}$ is the loss factor of the baseline matrix as measured in the experimental study, and the $\%SE_{filler}$ is the fractional strain energy stored in the filler at the $i^{th}$ orientation as calculated with the FEA solver

$$\eta_{effective-filler} = \frac{\eta_{composite} - \eta_{matrix}[1 - \frac{\sum_{i=0}^{\frac{\pi}{2}} \%(SE)_{filler}}{i}]}{\frac{\sum_{i=0}^{\frac{\pi}{2}} \%(SE)_{filler}}{i}} \quad (20)$$

This value while intrinsically high is product of the modeling techniques used, however, it does offer some significant insight to the behavior of the nanocomposite when subject to loadings resulting in activation of the frictional slip mechanism. The limiting feature of this model is the assumed perfect bonding of the filler and matrix, wherein this model does not account for the frictional slip, at the interphase region, associated with drastic damping augmentation, hence the large values for effective filler's loss factor, it should be noted that these values, while large, are good representation of effective filler loss factors, but should not be taken as intrinsic values given the limitation of the strain energy methods and nonlinear elastics associated with frictional energy dissipation. The geometry of high aspect ratio fillers allows for a shear stress buildup at the ends of the filler, with load, once a critical shear stress level is achieved de-bonding occurs and filler is allowed to slip relative to the matrix. In developing the model it was observed that at 1% strains in the material exhibited linear viscoelastic behavior, in fact linear elastic behavior was seen all the way up to 3.2% strain, however upon closer inspection there was actually de-bonding that was occurring, but it was recovered based on the Van der Waals bonds broken to allow for the slip. Future work will include smaller strain amplitude models and experimentation. However, at linear viscoelastic levels, before frictional sliding occurs; this model can serve to offer insight to the effect of the random orientation and filler waviness on the viscoelastic response in nanocomposites with high aspect ratio fillers as well as the intrinsic material properties of the fillers. Other modeling techniques have been used to attempt to get intrinsic values of the nanofiller loss factor, however these techniques, i.e. molecular

dynamics simulations, also fall short in developing usable numbers for modeling the viscoelastic response of the nano enhanced composites as they also do not account for the variations in nano filler geometry as seen in application. Looking to the future it would be beneficial to develop a model utilizing a both the intrinsic properties of the nano fillers as well as modifying elements reflective of the geometry limitations, coupled with a strain dependent frictional slip term. However, at the moment the combined modeling, analytical, and experimental approaches are best used to gain insight to the fundamental behavior while keeping in mind the limitations of the techniques used.

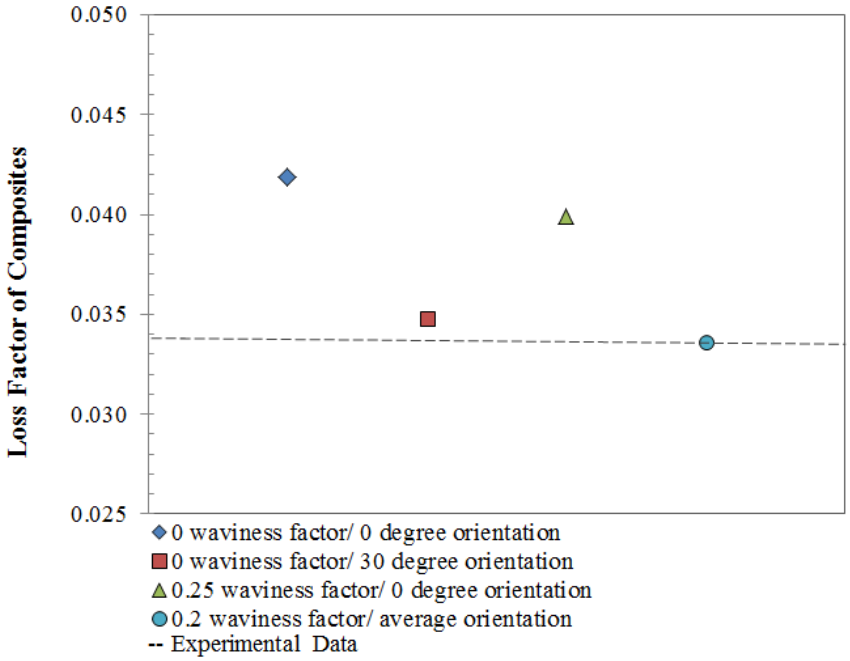


**Figure 28:** Calculated composite loss factor utilizing different modeling techniques (3wt% CNF filled composite FE model; filler loss factor is 0.53).

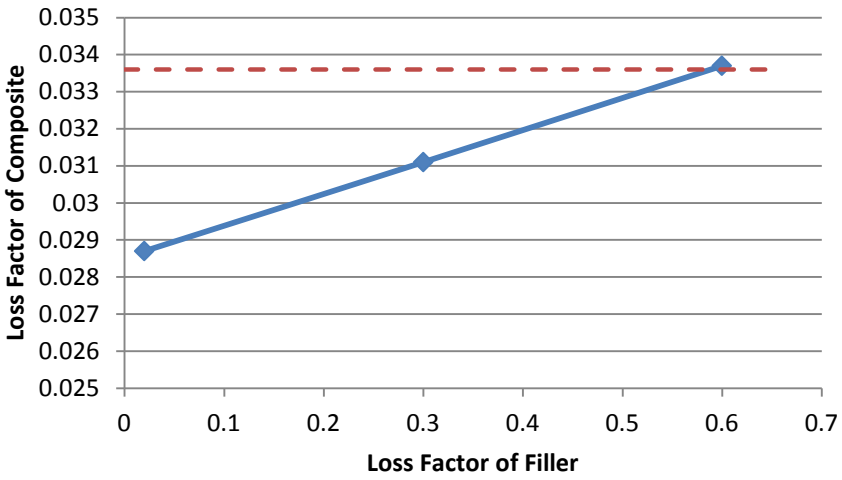


**Figure 29:** Calculated composite loss factor utilizing various assumed filler loss factors (3wt% CNF filled composite FE model; exp. data is 0.0336).

In this comprehensive study experimental, analytical and modeling techniques were used to look at the effect of filler waviness and orientation on the viscoelastic response of high aspect ratio filler nanocomposites. It was demonstrated, through the experimental inquiry, that the use of high aspect ratio fillers in nanocomposites can be used to significantly enhance the viscoelastic response of such composites, as well as the structural properties; as demonstrated by the enhanced composite loss factor and increased $T_g$ respectively. The results of the experimental investigation were then used to develop FEA models, used for a parametric inquiry as to the effect of filler orientation and waviness on the overall viscoelastic response of the nanocomposites. Here it was discovered that these two factors may account for much of the large performance gap seen between the experimental studies of high aspect ratio filler nanocomposites and conventional modeling techniques, which do not account for the inherent filler geometries and orientation in the nanocomposites. Concurrently, the experimental study and the FEA models were used in conjunction with analytical strain energy methods to characterize the effective constituent properties of the nano scale fillers, which is a matter of importance for the development of effective modeling techniques required to aid the development of the next generation of engineered materials. In looking at the results of the parametric inquiries it was discovered that filler waviness can contribute a 1.1% variation in the strain energy stored in the filler, over the studied spectrum; while filler orientation can contribute a 2.25%

variation in the strain energy stored in the filler for the filler loadings investigated. These variations while seemingly small can have significant implications in nanocomposite modeling where filler loadings are small; and fractional strain energy in the filler is also small, resulting in a wide variation of calculated filler properties for use in macro scale modeling, thus small changes can have significant impact in the composite performance and lead to the large discrepancies seen in conventional modeling techniques. Therefore, the need to carefully consider and understand the geometric limitations inherent in high aspect ratio filler nanocomposites as well as the limitations of the randomly oriented fillers seen in most nanocomposites has been studied in order to develop more useful modeling techniques which will reduce the performance gaps between predicted and experimental viscoelastic performance of high aspect ratio nanocomposites.

## 5. Conclusions

In this study a comprehensive look at damping in nanostructured composites has been presented, with detailed investigations on many of the key factors hypothesized to be critical to the overall damping performance seen in high aspect ratio nanocomposites. Specifically, investigations as to the effect of operating temperature, operating frequency, aspect ratio, multiple fillers, filler orientation, and filler waviness have been presented in detail.

In beginning this study, initial experimental investigations were made to validate the damping enhancement achievable with the use of high aspect ratio nano fillers such as CNF, here it was successfully shown that the use of CNF could provide broad spectrum passive damping enhancement to nano structured composites both as nano composites and as a nano enhanced or nanocomposite resin for fiber composites. In the DMA investigation of the nano composites it was shown that the storage modulus of the nano composites were increased with filler loading across all temperatures investigated. Similarly, the loss modulus was also increased with CNF filler loading across all temperatures investigated, which translated to an increased damping loss factor across all temperatures investigated. In addition to a 25% increase in the damping loss factor seen at 25°C and 1Hz test frequency, a 0.85°C shift in $T_g$ was noted with 5wt% filler loadings, indicating a reinforcement effect from the CNF filler. Investigations in to the frequency response of the nano composites showed similar trends to the temperature investigation for the storage modulus, where the

storage modulus was increased with filler loading across all frequencies investigated. However, in the loss modulus results it was discovered that while the loss modulus was increased with filler loading across all frequencies investigated, there was a distinct reduction shift in the loss modulus values at a frequency of 1Hz. This is hypothesized to be related to the intrinsic relaxation time of the material as it was also seen in the baseline. This trend also translated to the damping loss factor results where again a distinct reduction in the damping loss factor was seen at frequencies of 1Hz and above. Yet, in all cases the nanocomposites outperformed the baseline epoxy across all frequencies investigated. Following the initial DMA investigations, dynamic cyclic testing of the nanocomposites was performed at more realistic strains on larger samples. Again the CNF enhanced nanocomposites showed notable improvements in both storage and loss moduli, as well as damping loss factor, however in the investigation utilizing multiple strain levels a strong strain dependent response was noted, consistent with theories on randomly oriented fillers. Utilizing the initial DMA and dynamic cyclic testing results an analytical model, based on short fiber theory, modified for random filler distributions and complex constituent moduli was developed to look at damping in nanocomposites from an analytical perspective. Modeling was developed to look specifically at the effect of filler aspect ratio where the effect of filler aspect ratio was investigated both analytically and experimentally. It was discovered that while high aspect ratio fillers are required for damping enhancement, fillers with an aspect ratio beyond 100 exhibited a reduction in the damping enhancement provided both experimentally and analytically. Following the initial modeling validation and initial experimental results fiber composites were fabricated utilizing a nanocomposite resin, to make multiscale composites. Nano enhanced multiscale composites were successfully fabricated in 4, 6, and 8 ply unidirectional configuration. Beam specimens cut from the fiber composite panels were tested according to ASTM E-765-005 beam vibration testing where damping enhancement of up to 130.8% was seen in 6 ply 5wt% nano composite resin for mode II damping. Understanding that, much of the damping measured in the beam vibration testing was air damping attributed to the testing setup, dynamic cyclic testing was performed on the multiscale composite beams in order to eliminate the air damping effects and attempt to get a more fundamental insight into the damping enhancement achieved. Again strong strain dependent responses were observed for the multiscale beams in dynamic cyclic testing where a 47% improvement in damping

loss factor was observed for a 3wt% at1% applied strain, which was consistent with the dynamic cyclic testing performed on the nanocomposite specimens.

The next phase of this investigation looked at the effect of multiple nanoscale fillers, being that damping is often one of many specific requirements of engineered composites the idea of using multiple nanoscale fillers to tailor multiple functions in a material leads to questions about the impact of having multiple nanoscale fillers and the overall impact on the damping response. In this study nanocomposites were fabricated containing both CNF and $SiO_2$ nano particles. In looking at the DMA results for the multiple filler nanocomposites increases in storage modulus were seen across the spectrum at all temperatures and frequencies investigated for all filler loadings; similar results were seen in the loss modulus, however the most significant loss modulus gains were seen in the composites utilizing CNF, either alone or in conjunction with the $SiO_2$, leading to the conclusion that the high aspect ratio fillers are better suited to damping applications. The use of multiple fillers led to the expansion of the previously developed model in order to look at multiple fillers from an analytical perspective. As well with the different geometry and material properties, this model allowed for a simultaneous investigation to both aspect ratio and filler material properties. In looking at the modeling results the analytical performance overstated the experimental performance in all instances that contained CNF filler. Upon closer examination of the results it was discovered that the reinforcement effect of the CNF was being overstated by the model, underscoring the need for the ability to accurately measure constituent material properties. Following this discovery a semi-empirical model was developed utilizing measured CNF nanocomposite material properties input for the matrix and treating the $SiO_2$ as filler. This produced much closed results having only a 1.3% and 8.35% discrepancy in storage and loss modulus respectively. Noting the discrepancy caused by the overstated reinforcement effect of the CNF filler, the need to better understand the factors affecting the reinforcement were studied in detail.

The final investigation of this study looked at the effect of both filler orientation and waviness. A comprehensive experimental, FEA, and analytical approach, utilizing strain energy methods to look at the effect of both filler orientation and waviness were developed. As well, these techniques utilized allowed for an effective filler loss factor to be backed out when used in conjunction with experimental results,

which proved to offer substantial insight to material properties which are traditionally difficult to obtain given the size of the filler. In analyzing the FEA results it was discovered that a small amount of filler waviness may actually serve to enhance load transfer capabilities and thereby structural performance of the composite. In applying the strain energy methods along with the FEA results it was discovered that filler orientation contributed up to a 2.2% variation in the fractional strain energy stored in the filler, while waviness contributed up to a 1% variation in the fractional strain energy stored in the filler. While these variations are seemingly small the fact that a majority of the strain energy stored in a composite is in the more compliant matrix, small variations in the fractional strain energy stored in the filler can lead to large variations in the predicted performance generated by an analytical model, highlighting the need to consider filler orientation and waviness issues when developing analytical models.

## 6. Future work

It has been clearly shown that the use of a high aspect ratio nanoscale filler can serve to provide a broad spectrum passive damping enhancement, however the greatest limiting factor preventing this technology from application is the need for design useful models, which can be used to accurately predict and engineer both damping and structural performance. Many of the issues preventing these models are attributed to the issues that arise in obtaining accurate material properties for nanoscale fillers, which are not obtainable by conventional testing means. The next evolution of this work will focus on in-situ nano composite measurements and modeling techniques that allow for a better fundamental understating of high aspect ratio nano filler material properties. Utilizing more accurate fundamental material properties for the filler phase of the nanocomposites will allow for a more fundamental, generalized design model that will allow for better engineered nano composites capable of meeting the challenges of the next generation of engineered materials.

## References


1. Gibson, Ronald F. *Principles of Composite Material Mechanics*. 2nd ed. Boca Raton: CRC Press, 2007. 1-22, 518-40.
2. Suhr, Jonghwan, Nikhil Koratkar, Pawel Keblinski, and Pulickel Ajayan. "Viscoelasticity in Carbon Nanotube Composites." *Nature Letters* 4: 134-37.
3. Koratkar, Nikhil, Jonghwan Suhr, Amit Joshi, Ravi S. Kane et al. "Characterizing Energy Dissipation in Single-Walled Carbon Nanotube Polycarbonate Composites." *Applied Physics Letters* 87: 63102.
4. Zhou, X, Eungsoo Shin, K W. Wang, and C E. Bakis. "Interfacial Damping Characteristics of Carbon Nanotube Based Composites." *Composites Science and Technology* 64: 2425-37.
5. Rao, Mohan D. "Recent Applications of Viscoelastic Damping for Noise Control in Automobiles and Commercial Airplanes." *Journal of Sound and Vibration* 262: 457-74.
6. Kireitseu, Maksim, David Hui, and Geoffrey Tomlinson. "Advanced Shock Resistant Vibration Damping of Nanoparticle Reinforced Composite Material." *Composites Part B: Engineering* 4 Mar. 2007.
7. Gibson, Ronald F., Emmanuel O. Ayorinde, and Yuan-Feng Wen. "Vibrations of Carbon Nanotubes and their Composites: A Review." *Composites Science and Technology* 67: 1-28.
8. Tanimoto, Toshio. "A New Vibration Damping CFRP Material with Interlayers of Dispersed Piezoelectric Ceramic Particles." *Composites Science and Technology* 67: 213-21.
9. Blackwell, Christopher M, The Evaluation of the Damping Characteristics of a Hard Coating on Titanium, 2002, Master's thesis, Air Force Institute of Technology
10. Rao, Mohan D, Recent Applications of Viscoelastic Damping for Noise Control in Automobiles and Commercial Airplanes, *Journal of Sound and Vibration* ***2003***, 262, 457-74.
11. Lincoln DM, Vaia RA, Brown JM, Benson-Tolle TH. Revolutionary nanocomposite materials to enable space systems in the 21st century. *IEEE Aerospace Conf Proc*. 2000: 183-192.
12. Koratkar, N., Jonghwan S., Amit J., Ravi S. K. et al. Characterizing Energy Dissipation in Single-Walled Carbon Nanotube Polycarbonate Composites, *Applied Physics Letters* ***2005***, 87, 63102.
13. Zhou, X, Eungsoo S., K W. Wang, and C E. Bakis. Interfacial Damping Characteristics of Carbon Nanotube Based Composites, *Composites Science and Technology* ***2004***, 64, 2425-37.
14. Kireitseu, M., David H. and Geoffrey T., Advanced Shock Resistant Vibration Damping of Nanoparticle Reinforced Composite Material, *Composites Part B: Engineering* ***2007***, 4 Mar.
15. Suhr, Jonghwan, Nikhil Koratkar, Pawel Keblinski, and Pulickel Ajayan. "Viscoelasticity in Carbon Nanotube Composites*." Nature Letters* 4: 134-37.
16. Yao, X F., H Y. Yeh, D Zhou, and Y H. Zhang. "The structural characterization and properties of SiO2 -epoxy nanocomposites." *Journal of composite materials* 40: 371-81.
17. Zheng, Yapping, Rongchang Ning, and Ying Zheng. "Study of SiO2 nanoparticles on the improved performance of epoxy and fiber composites." *Journal of reinforced Plastics and Composites* 24: 223-33.
18. Kontou, E, and M Niaounakis. "Thermo-mechanical properties of LLDPE / $SiO_2$ nanocomposites." *Polymer* 47: 1267-80.
19. Natsuki, Toshiaki, Qing-Qing Ni, and Shi-Hong Wu. "Temperature Dependence of Electrical Resistivity in Carbon Nanofiber / Unsaturated Polyester Nanocomposites." *Polymer Engineering and Science* (2008).
20. Finegan, Ioana C., Gary G. Tibbetts, and Ronald F. Gibson. "Modeling and characterization of damping in carbon nanofiber / polypropylene composites." *Composites Science and Technology* 63 (2003): 1629-35
21. Adams, Donald F., Leif A. Carlsson, and R. Byron Pipes. *Experimental Characterization of Advanced Composite Materials*. Third ed. Boca Raton: CRC Press, 2002. 143-68.
22. Scott, C., H. Ishida, and F.H. J. Maurer. "Melt State Dynamic Mechanical Properties of Polyethylene/EPDM/Silicon Dioxide Composites." *Journal of Reinforced Plastics and Composites* 10 (1991): 463-76.

23. Wei, Chenyu, and Deepak Srivastava. "Nanomechanics of carbon nanofibers: Structural and elastic properties." *Applied Physics Letters* 85.12 (2004): 2208-10.
24. Fisher, F.T., Bradshaw, R.D., and Brimson, L.C. “Effects of Nanotube Waviness on the Modulus of Nanotube-Reinforced Polymers” *Applied Physics Letters* 80 (2002) 4647.
25. C. T. Sun, *Proceedings of the American Society for Composites, Seventeenth Technical Conference*, Published by CRC Press, 2002
26. Fisher, F T., R D. Bradshaw, and L C. Brinson. "Fiber waviness in nanotube-reinforced polymer composites - I: Modulus predictions using effective nanotube properties." *Composites Science and Technology* 63 (2003): 1689-703.
27. Shi, Dong-Li, Yonggang Y. Huang, Keh-Chih Hwang, and Huajian Gao. "The Effect of Nanotube Waviness and Agglomeration on the Elastic Property of Carbon Nanotube-Reinforced Composites." *Journal of Engineering Materials and Technology* 126 July (2004): 250-57.
28. Li, Cyunyu, and Tsu-Wei Chou. "Failure of carbon nanotube / polymer composites and the effect of nanotube waviness." *Composites: Part A* 40 (2009): 1580-86. Print.
29. Takeda, Tomo, Yasuhide Shindo, Yu Kuronuma, and Fumio Narita. "Modeling and characterization of the electrical conductivity of carbon nanotube based polymer composites." *Polymer* 52 (2011): 3852-56.
30. Yazdchi, K., and M. Salehi. "The effects of CNT waviness on interfacial stress transfer characteristics of CNT/polymer composites." *Composites: Part A* 42 (2011): 1301-09.
31. Sheng Tian Æ Xiaodong Wan Fabrication and performances of epoxy/multi-walled carbon nanotubes/piezoelectric ceramic composites as rigid piezo-damping materials” *Journal of Material Science* (2008) 43:4979–4988.
32. Luo, Dongmei, Wen-Xue Wang, and Yoshihiro Takao. "Application of Homogenization Method on the Evaluation and Analysis of the Effective Stiffness for Noncontinuous Carbon Nanotube/Polymer Composites." *Polymer Composites* (2007): 688-95.
33. Sanada, Kazuaki, Yoshihiro Takada, Shunki Yamamoto, and Yasuhide Shindo. "Analytical and Experimental Characterization of Stiffness and Damping in Carbon Nanocoil Reinforced Polymer Composites." *Journal of Solid Mechanics and Materials Engineering* 2.12 (2008): 1517-27. Print
34. Joshi, Unnati A., Satish C. Sharma, and S P. Harsha. "Effect of waviness on the mechanical properties of carbon nanotube based composites." *Physica E* 43 (2011): 1453-60.
35. Unger, Eric E., and Edward M. Kerwin. "Loss Factors of Viscoelastic Systems in Terms of Energy Concepts." *Journal of the Acoustical Society of America* 34.7 (1962): 954-57.
36. Iijima, S. “Helical Microtubes of Graphitic Carbon.” *Nature* 354 (1991): 56-58.
37. Qian, D., Wagner, G.J., Liu, W. K., Yu, M.F. and Ruoff, R.S. “Mechanics of Carbon Nanotubes.” *Applied Mechanics* 55 (2002): 495-533.
38. Zhang, P., Huang, Y., Geubelle, P. H., Klein, P.A., and Hwang, K.C., “The Elastic Modulus of of Single-Wall Carbon Nanotubes: A Continuum Analysis Incorporating Interatomic Potentials.” *International Journal of Solid Structures* 39 (2002): 3893-3906.
39. Yao, Z.H., Zhu, C.C., Cheng, M., and Liu, J. “Mechanical Properties of Carbon Nanotube by Molecular Dynamics Simulation.” *Computational Materials Science* (2001): 180-84.
40. Thostenson, E.T., Ren, Z., and Chou, T.W. “Advances in the Science and Technology of Carbon Nanotubes and Their Composites: A Review.” *Composites Science and Technology* 61 (2001): 1899-1912.
41. Bower, C., Rosen, R., Jin, L., and Zhou, O. “Deformation of Carbon Nanotubes in Nanotube- Polymer Composites.” *Applied Physics Letters* 74 (1999): 3317-19.
42. Andrews, R., Jacques, D., Rao, A. M., Rantell, T., Derbyshire, F., Chen, Y., Chen, J., and Haddon, R.C. “Nanotube Composite Carbon Fibers.” *Applied Physics Letters* 75 (1999): 1329-31.
43. Andrews, R., Jacques, D., Minot, M., and Rantell, T. “Fabrication of Carbon Multiwall Nanotube / Polymer Composites by Shear Mixing.” *Macro-molecular Materials and Engineering* 287 (2002): 395-403.
44. Qian, D., Dickey, E.C., Andrews, R., and Rantell, T. “Load Transfer and Deformation Mechanisms in Carbon Nanotube-Polystyrene Composites.” *Applied Physics Letters* 76 (2000): 2868-70.

45. Xu, L.R., and Sengupta, S. “Interfacial Stress Transfer and Property Mismatch in Discontinuous Nanofiber / Nanotube Composites.” *Journal of Nanotechnology* 5 (2005): 620-26.
46. Li, X., Gao, H., Scrivens, W.A., Fei, D., Xu, X., Sutton, M.A. et al. “Nanomechanical Characterization of Single Walled Carbon Nanotube-Reinforced Epoxy Composites.” *Nanotechnology* 15 (2004): 1416-23.
47. Shi, D.L., Feng, X.Q., Huang, Y.G.Y., Hwang, K.C., and Gao, H.J. “The Effect of Nanotube Waviness and Agglomeration on the Elastic Property of Carbon Nanotube Reinforced Composites.” *Journal of Engineering Material Technology* 126 (2004): 250-57.
48. Thostenson, E.T., and Chou, T.W. “On the Elastic Properties of Carbon Nanotube Based Composites: Modeling and Characterization.” Physics D: *Applied Physics* 36 (2003): 573-82.
49. Chandra, R., Singh, S.P., and Gupta, K. “Micromechanical Damping Models for Fiber Reinforced Composites: A Comparative Study.” *Composites Part A* 33 (2002): 787-796.
50. Liu, Y.J., and Chen, X.L. “Evaluations of the Effective Material Properties of Carbon Nanotube Based Composites Using Nanoscale Representative Volume Element.” *Mechanics of Materials* 35 (2003): 69-81.
51. Chun, H.J., Shin, J.Y., and Daniel, I.M. Effect of Material Geometric Nonlinearities on the Tensile and Compressive Behavior of Composite Materials with Fiber Waviness. *Composites Science and Technology* 61 (2001): 125-34.